THE EFFECTS OF CAPILLARY PLATES ON VAPOUR-LIQUID EQUILIBRIUM IN AQUEOUS ALCOHOL SYSTEMS

by

Nga Sze Judy Wong

Department of Chemical Engineering

McGill University, Montreal

April, 1997

A thesis submitted to the Faculty of Graduate Studies and Research in partial fulfillment of the requirements for the degree of Master of Engineering,

ABSTRACT

Vapour-liquid equilibrium is the driving force behind many separation processes such as distillation. Previous studies have shown that the vapour-liquid equilibria of many mixtures can be altered when the vapour-liquid interface is modified by capillary systems. This thesis studied the effects of capillary actions due to modified vapour-liquid interfaces on the vapour composition of ethanol-water and 1-propanol-water systems. A method was developed to measure and compare the vapour compositions of systems with a planar vapour-liquid interface and systems with capillary plates. Experiments were conducted to investigate the effects of interface materials, pore sizes and liquid compositions. Significant differences in vapour composition between capillary systems and systems with a planar interface were observed. This difference was much larger than that predicted by the Kelvin equation. The mechanism of the capillary actions and the factors causing the increase in vapour composition were investigated.

RÉSUMÉ

L'équilibre liquide-vapeur est la force matrice impliquée dans de nombreux procédés de séparation tels que la distillation. De précédentes études ont montré que les équilibres liquide-vapeur de nombreux mélanges peuvent être perturbés lorsque l'interface liquide-vapeur est modifiée par des systèmes capillaires. Cette étude porte sur les effects des phénomènes capillaires dus à des interfaces liquid-vapeur modifiées, sur la composition de la vapeur de mélanges éthanol-eau et 1-propanol-eau. Une méthode a été développée pour mesurer et comparer la composition de la vapeur des systèmes ayant, soit une interface liquide-vapeur plane, soit des disques capillaires. Les expériences ont été réalisées afin de déterminer l'influence des matériaux de l'interface, de la taille des pores, ainsi que celle de la composition des liquides. Des différences significatives dans la composition de la vapeur ont été observées entre les systèmes capillaires et les systèmes avec interface plane. Cette différence était nettement plus importante que celle prévue par l'équation de Kelvin. Le mécanisme de l'action capillaire et les facteurs provoquant l'augmentation de la composition de la vapeur ont été étudiés.

ACKNOWLEDGMENTS

My outmost gratitude to Dr. Jana Simandl for her guidance and inspiration. The advice and ideas of Dr. M.E. Weber, Dr. J.H. Vera and the research group are much appreciated. I would like to thank Douglas Quong and my family for their continual support and encouragement. The financial support of the Natural Sciences and Engineering Research Council (NSERC), McGill University's Chemical Engineering department and the Brace Research Institute are gratefully acknowledged. Samples of sintered metal plates were generously provided by Pall Canada and Newmet Kresöge.

TABLE OF CONTENTS

LIST OF TABLES

Table

1.0 INTRODUCTION

Vapour-liquid equilibrium (VLE) is defined as the state of a closed system when the diffusion of the liquid into the vapour occurs at the same rate as the diffusion of the vapour into the liquid. This equilibrium is the driving force behind many separation processes such as distillation and extraction.

There are certain limitations on the thermodynamics equilibria that can be achieved and one that commonly exists is an azeotrope. When the vapour pressure of pure compounds are close to one another in a mixture, the mixture may form an azeotrope where the liquid and the vapour have the same composition at its boiling point (Perry, 1984). Since the location of the azeotrope is dependent on the pressure of the system, separation of a mixture using simple distillation may not be possible for a range of pressures.

Approaches to VLE modification that are used commercially are pressure changes and solvent addition. The alteration of pressure in the system may not be practical due to equipment and economical constraints especially when large columns with high numbers of plates are required (Wankat, 1988). Solvent addition used in extractive distillation and azeotropic distillation can be effective in separating the mixture but this elevates process operation costs. An alternative to these conventional methods is capillary distillation which alters the VLE through modification of the vapour-liquid interface (Yeh *et al.* 1991a).

A study by Yeh *et al.* (1986) has shown that the VLE of a system where the

vapour-liquid interface is modified by porous metal plates is different from that of solutions with a planar interface. A shift in the azeotropic composition of the ethanol/water system to a higher value was also observed.

This master's thesis is a report on the effects of vapour-liquid interface modifications on the VLE of ethanol/water and propanol/water mixtures. The capillary surface modifiers tested were sintered stainless steel plates, fritted glass filters and a Durapore membrane. A method was developed to measure the vapour compositions of the modified system and of the bulk solutions. The term bulk solution refers to a system where the vapour-liquid interface is not modified. Factors such as equilibrium time, liquid volume, pore size and liquid compositions were studied.

A review of past research on capillary systems and related papers is presented in chapter 2 of this thesis. Chapter 3 describes the apparatus design, equipment set-up and experimental methods. The results of the experiments with various capillary surface modifiers are discussed in chapter 4. Conclusions and recommendations are presented in chapter 5.

2.0 LITERATURE REVIEW

2.1 Thermodynamics of Vapour-Liquid Equilibrium in Capillaries

The Kelvin equation

$$\ln \frac{p'}{p^o} = \pm \frac{2\,\sigma\,v''}{R\,T\,r} \qquad (2.1)$$

has been widely used to predict the vapour pressure p' over a curved surface with radius of curvature r, surface tension σ and molar volume v'' where p° is the vapour pressure of the system over a flat surface at temperature T (Defay and Prigogine, 1966). However, studies by Coleburn *et al.* (1971) have shown that vapour pressure lowerings of water, isopropyl alcohol and toluene in capillaries are many times larger than the predicted values. The vapour pressure and the equilibrium radii of the meniscus of toluene held in capillaries of a few microns in diameter were measured. The vapour pressures were used in the Kelvin equation to back calculate the equilibrium radii. The observed radii were 10 to 30 times larger than those predicted by the Kelvin equation. This means that there is significant lowering in vapour pressure even at larger radii. The authors postulated that this may be due to the formation of toluene layers at the capillary walls with modified physical properties such as surface tension and density which are not taken into account by the Kelvin equation.

To compensate for the inadequacy of the Kelvin equation, modifications to the equation were made or new equations were proposed to predict the vapour

pressure. The approach to vapour pressure prediction over curved surfaces was through a thermodynamic analysis performed on systems in a gravitational field that can be applied to pendant or sessile drops, liquid lenses and fluids in porous media. The mechanical and physicochemical phenomena were discussed along with changes in equilibrium (Boucher, 1984). The vapour pressure p of a component of a phase separated from a liquid phase by a curved surface was described by:

$$RT \ln(\frac{p}{p^o}) = -(\rho^l - \rho^v)\, gzv^l + (p - p^o)\,(v^l - B) \qquad (2.2)$$

where v^l refers to the partial volume of one of the component, ρ is the density of the particular phase (liquid or vapour) and p° is the vapour pressure above a plane surface. The non-ideality of the vapour is incorporated into the equation by the use of the virial coefficient B. g is standard gravity and z is the height of the liquid. R is the gas constant and T is the temperature of the system.

Boucher (1990) developed a modified version of the Kelvin equation to improve its prediction of vapour pressures in capillary systems. In his model, the vapour pressure of the solvent is proportional to the interface curvature due to Kelvin's effect but the solute contributes to the lowering of the solvent vapour pressure according to Raoult's law. Thermodynamic expressions pertaining to the vapour pressure of solutions over capillary-condensed curved surfaces have been derived taking into account interfacial tension, adsorption and curvature.

Using a surface thermodynamic approach, a general form of an alternate vapour pressure equation for vapour-liquid interfaces was developed (Kuz, 1991):

The properties of the fluid held in capillary systems may be difficult to measure when the pores approach molecular scale. Phase equilibrium metastability causes hysteresis loops in the adsorption isotherms which can be observed in the behaviour of fluids in porous media. Panagiotopoulos (1987) applied the Monte Carlo simulation in the Gibbs ensemble to the study of capillary condensation and adsorption behaviour of fluids in the narrow cylindrical pores for the direct determination of phase equilibria.

The wetting behaviour of a liquid contributes to solid-liquid interactions in a way that cannot be ignored in capillary systems or in thin films. At equilibrium, the chemical potential differs from that of a bulk liquid due to four types of solid-liquid interactions: compression of the electrostatic double layers within the film, the dispersion force, the resultant forces of overlapping adsorbed layers and the overlapping of boundary layers of liquids (Troung and Wayner Jr., 1987). These effects are assumed to be influential for the solid-liquid interface in capillaries.

In the design of experiments for the study of curved surfaces, it is useful to know the degrees of freedom in the system. It was found by Li (1994) that Gibbs' phase rule cannot be applied to these systems because the presence of curved surfaces decreases the number of mechanical equilibrium constraints which in turn increases the degrees of freedom. The number of degrees of freedom is different for moderately curved surfaces (radius of curvature in the order of millimetres) and highly curved surfaces (radius of curvature in the order of microns). The number of degrees of freedom for highly curved surfaces is suggested by:

$$f = 2S + 8 + r + 1 - N \quad (2.4)$$

where S is the number of highly curved interface phases, r is the number of chemical components and N is the number of pressure equality relations between bulk phases (Li, 1994).

The factors mentioned above explain the differences in vapour-liquid equilibrium (VLE) between capillary systems and bulk solutions. These differences have been observed in experimental studies and they may be strategically applied to the separation of non-ideal mixtures.

2.3 Experimentally Tested Systems

Capillary distillation is a method based on the fact that physical properties such as surface tension, density, viscosity and vapour pressure of liquids in small capillaries and pores are different from the properties in bulk solutions.

Yeh *et al.* (1986) studied an ethanol-water system held in capillary plates. The vapour pressure ratio of ethanol to water was increased by a factor of 1.58 over the values found in bulk solutions. Since relative volatility α is a ratio of vapour pressures, α was also increased 1.58 times. The azeotrope in bulk ethanol-water systems exists at an ethanol mole fraction of 0.906 at 50°C. However, when the solution was contained in the capillary plates, the azeotrope moved to a mole fraction of 0.9868 ethanol at the same temperature. These researchers also conducted experiments with other aqueous-organic systems and most systems showed an increase in relative volatility when compared with that of the bulk solutions (Yeh

et al., 1991b). The lowering of vapour pressures when liquid is held in small pores was attributed to not just the curvature of the meniscus, but also to induction force polar interactions and the London force dispersion interactions in the liquids (Yeh *et al.*, 1986). The Kelvin equation did not accurately predict the vapour pressure of polar liquids held in capillaries with radii in the order of microns. The explanation given was that at such small capillary radii, both the molecular interactions at vapour-liquid interfaces and at the solid-liquid interfaces must be taken into consideration.

The concept of capillary condensation for separation was applied to the separation of methanol-hydrogen in ceramic membranes (Sperry *et al.*, 1991). The methanol condenses in the pores of the membrane while the hydrogen gas diffuses through the pores. The vapour pressure reduction in the membrane was observed to be an order of magnitude larger than that predicted by the Kelvin equation. Dissolved salts enhance induced-dipole interactions between the pore walls and higher adsorbed layers that result in greater adsorption at the walls. The authors postulated that the failure of the Kelvin equation to predict the vapour pressure without correction factors is due to the unaccounted for non-ideality of condensable vapour, compressibility of condensate and adsorption on the pore walls. However, H_2 gas has been observed to diffuse through solids and not just through the pores. This is another possibility that may have an affect on the rate that hydrogen gas travels through the membrane.

Many different factors have been suggested as contributors to the lowering of vapour pressures in capillaries. The system is complicated by curvature, surface

tension, adsorption and different interface properties. Differences in vapour pressures have been experimentally observed in systems of small capillaries and sintered metal plates. This study developed a method to measure and compare the vapour compositions of capillary systems composed of metal sintered plates and fritted glass plates with the vapour composition of the bulk solutions. The pores in these structures are similar to those in membranes and thus the method was also applied to them.

3.2 Vial Design

Since vessels of a specific size are required for the autosampler of the gas chromatograph, the closed system was designed to accommodate the capillary plates while maintaining the same outer dimensions as regular sample vials.

The housing consisted of two fused sample vial tops with a porous plate held in the middle (Figure 3.1). The gap between the outer edge of the plate and the glass was sealed with silicon. This created the housing for the sintered metal plates and the fritted glass plates. To mount the membranes, a perforated metal plate was held in place in the same manner as the metal and glass plates. The membrane was cut to the same size as the perforated plate, placed on top of it and its edges sealed with silicon. The porous plates each had a diameter of 1.99cm. The total volume of the vial is 22ml. To ensure adequate vapour space for the autosampler needle, the vapour volume in the vial was designed to be 12ml while the liquid volume was 10ml.

The vials were made of pyrex glass which made them durable and allowed for the monitoring of the liquid level. Liquid level adjustments were made with a syringe through the bottom septum. The vapour sample was taken through the top septum. The vials were readily cleaned and reused. Since the septa used were specifically designed for the vials, the housing maintained a tight seal.

The plates were cleaned thoroughly before each run with acetone and distilled water and dried to ensure that there were no impurities in the system.

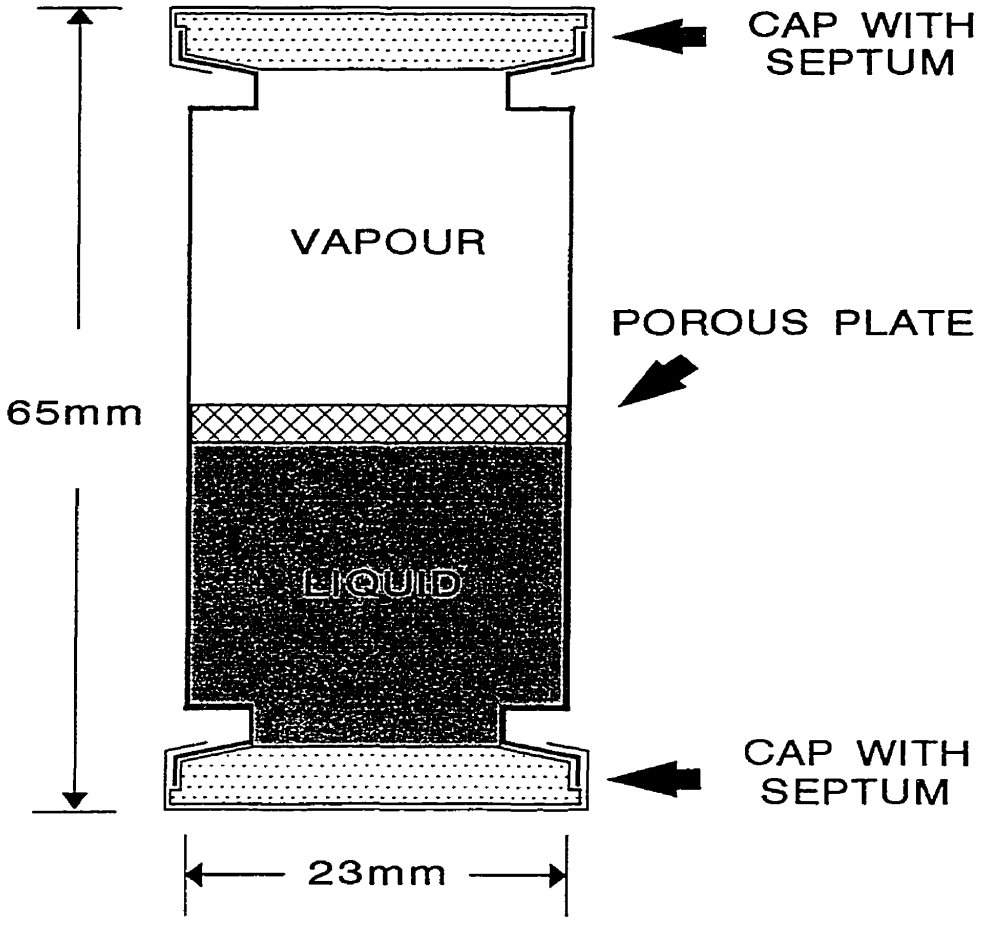

Figure 3.1: Housing unit for capillary plates.

3.3 Determination of Minimum Equilibrium Time

To ensure that the sample had reached equilibrium, several vials with bulk solution were heated for different lengths of time and the vapour composition measured. The resulting peak areas were plotted against the equilibration times (Figure 3.2). As indicated by the data points between time zero and 120 minutes, the vapour compositions did not have good reproducibility because the samples had not reached equilibrium. The equilibrium time should be at or above the time required for the curve to plateau. From Figure 3.2, the minimum equilibrium time was found to be 300 minutes for solutions with a planar interface.

For vials modified with porous plates, a longer time was required because of longer diffusion paths. Therefore, an equilibrium time of 24 hours was chosen.

3.4 The Sample Path

The liquid was allowed to equilibrate with the vapour in the sample vial without mixing or agitating. The vapour compositions of the alcohol/water systems were measured using a Genesis Headspace Autosampler and a Varian 3400 gas chromatograph (GC). The experimental set-up is illustrated in Figure 3.3.

The parameters of the headspace autosampler were manually programmed. The vapour pressure built up in the vial headspace forced a sample of the vapour through the sample loop. In this study, no pressurization gas was used in order to avoid dilution of the vapour space. Since the vials were not pressurized, the needle and the sample loop could not be flushed by the pressurization gas between runs.

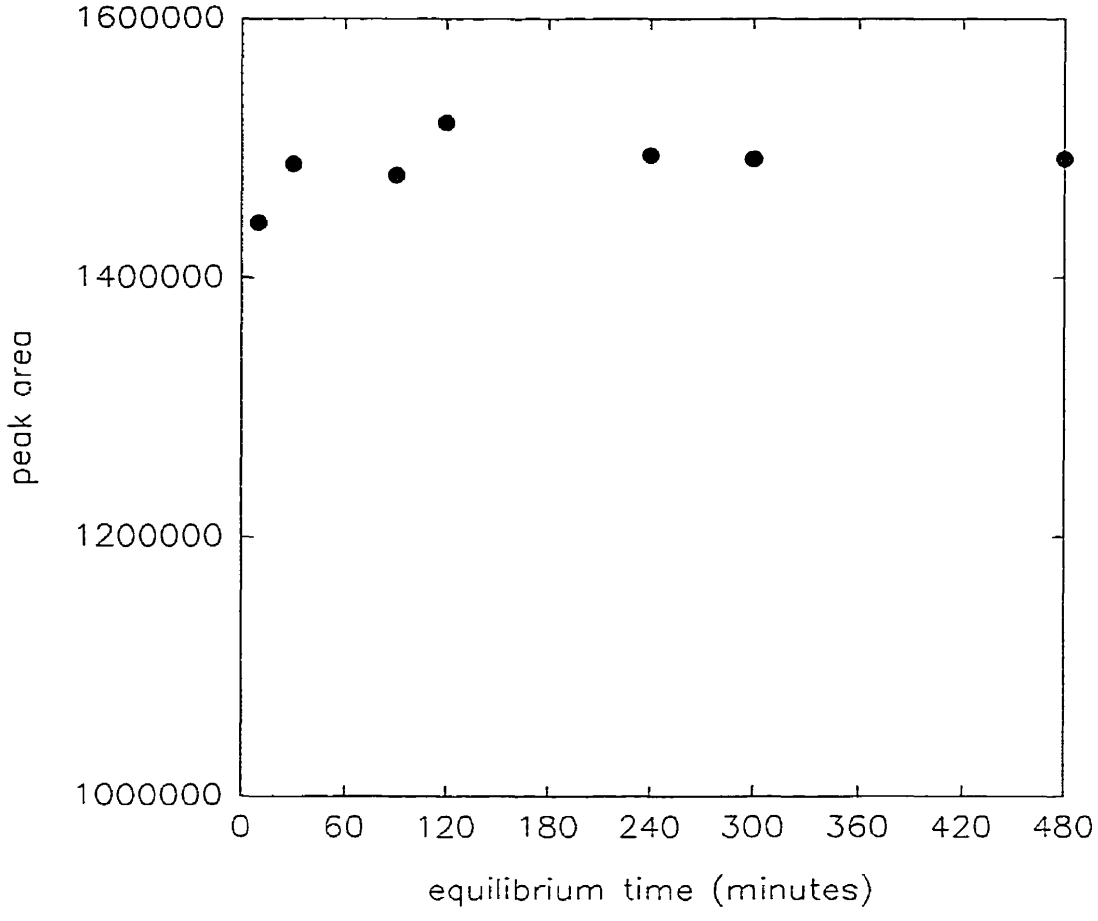

Figure 3.2: Determination of minimum equilibrium time for bulk ethanol/water solution at x_{EtOH} =0.4 and 60°C.

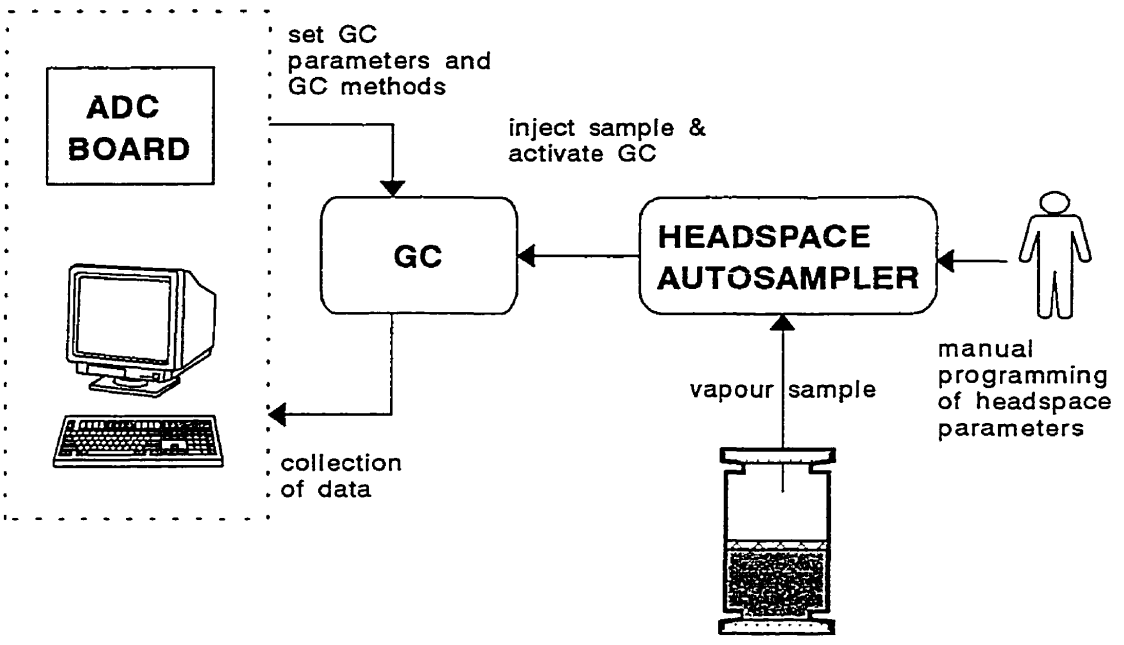

Figure 3.3: The experimental set-up.

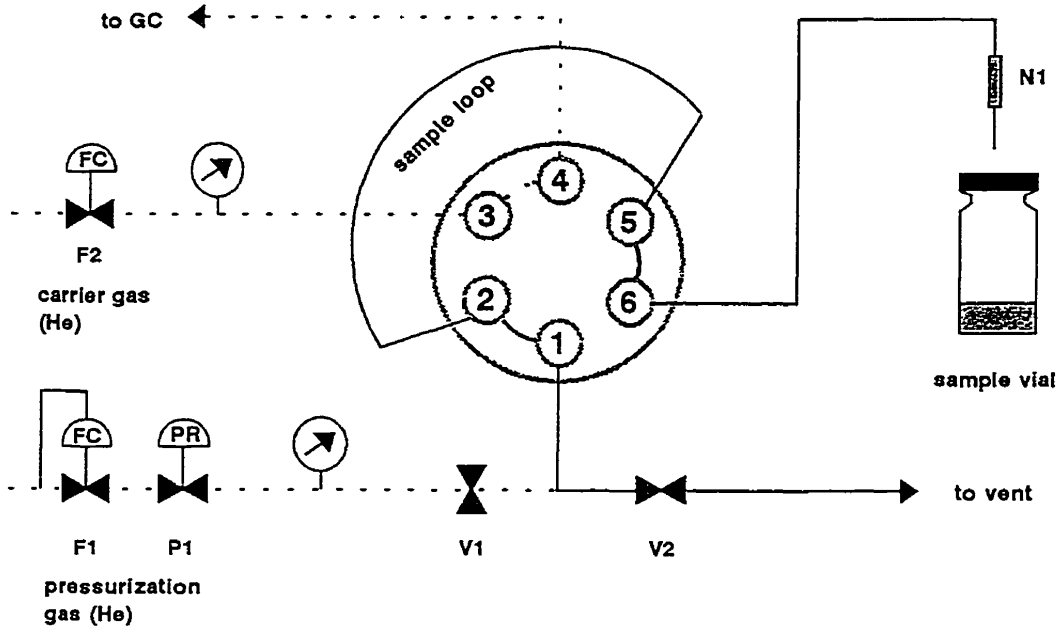

Figure 3.4: The autosampler configuration for the filling of sample loop.

3.5 Equipment Used

Specifications for the headspace autosampler and the gas chromatograph are listed in Tables 3.1 and 3.2 respectively. Table 3.3 records the types of capillary plates tested along with their nominal pore sizes and the suppliers. The chemicals used are specified in Table 3.4.

Table 3.1: Headspace autosampler specifications.

Headspace Autosampler	
Model	Genesis Headspace Autosampler with 50-position carrousel
Injector inlet connection	septum needle adaptor
Carrier gas	ultra high purity helium (Matheson)
Sample vial size	22ml vials (9 and 12ml vials may be used with platen sleeves and carrousel collar)
Sample loop volume	20μL

Table 3.2: Gas chromatograph specifications.

Gas Chromatograph	
Model	Varian 3400 Gas Chromatograph
Detector	Flame Ionization Detector (FID)
Column	DB-624 glass capillary column, length=75m, diameter=530μm
Make-up Gas	helium

Table 3.3: Capillary plates' specifications.

Capillary Plates		
type	nominal pore size	supplier
sintered stainless steel	3μm, 5μm, 10μm, 40μm	Newmet Kresõge
fritted glass	fine (4-8μm), medium (10-20μm)	Ace glass
Polyvinylidene fluoride hydrophobic Durapore membrane filters	0.45μm	Millipore

Table 3.4: Chemicals.

Chemicals		
product	purity	supplier
ethyl alcohol	anhydrous	Commercial Alcohols
1-propanol	Accusolv	Anachemia
acetone	lab grade	Anachemia
distilled water	---	---

3.6 Experimental Procedures

For each set of runs at a certain liquid composition, modified vials with plates were prepared along with at least three vials without any plates. This served as a calibration for any variations in run conditions that would affect the peak area. The vials were filled at room temperature and they were not evacuated. They were placed into the platen of the headspace autosampler which was at a constant temperature of 60.0±0.2°C. Due to thermal expansion of the liquid, the liquid level was adjusted after 90 minutes to ensure the liquid was below the top surface of the plate. This was carried out by removing the vials from the platen and withdrawing the excess liquid with a syringe from the bottom septum. The vials were returned to the platen and allowed to reach equilibrium for 24 hours before sampling.

3.7 Headspace Autosampler and GC Parameters

By testing various instrument settings, the analytical method which yielded the most reproducible data determined. It was used for all subsequent experiments. Table 3.5 lists these parameters for the ethanol/water system and the 1-propanol/water system.

Table 3.5: Parameters used for ethanol and propanol composition determination.

	Ethanol	1-Propanol
Headspace autosampler:		
Platen temperature	60°C	60°C
Equilibrium time	24 hrs	24 hrs
Pressurization time	0.00 min	0.00 min
Pressure equilibration time	0.00 min	0.00 min
Loop fill time	0.25 min	0.25 min
Loop equilibrium time	0.30 min	0.30 min
Inject time	2.00 min	2.00 min
Line temperature	175°C	175°C
Valve temperature	175°C	175°C
Gas chromatograph:		
Column temperature	65°C	65°C
Injector temperature	140°C	140°C
Detector temperature	250°C	250°C
	The column was ramped to 120°C and held for 2 minutes at that temperature after each 5.50 minute run to prevent carry over between samples	The column was ramped to 120°C and held for 2 minutes at that temperature after each 5.50 minute run to prevent carry over between samples

4.2 Conversion of Peak Area to Mole Fraction

After the equilibrium time established in the previous chapter was attained, the vapour in the vial reached the equilibrium mole fraction corresponding to the liquid mole fraction from vapour-liquid equilibrium (VLE) data. The Peng-Robinson-Stryjek-Vera equation of state (PRSV) was used to generate VLE data for the ethanol/water system at 60°C. A program written in MATLAB was used to perform the iterations (Appendix B). The VLE values were in good agreement with the published data of Udenkov *et al.* (1952) (Figure 4.1). The curve generated by the PRSV equation of state was used as the basis to convert gas chromatograph peak area values to vapour mole fraction.

The area under the peak from the GC output is directly proportional to the concentration of the alcohol in the sample but it cannot be directly converted to a mole fraction. The mole fraction of alcohol in the headspace is defined in equation 4.1 as

$$alcohol\ mole\ fraction = \frac{moles\ of\ alcohol\ in\ vapour}{total\ moles\ of\ gas} \qquad (4.1)$$

Since water and air do not show up in the GC output, the total moles of gas in the sample was unknown.

The vapour compositions of solutions with different liquid mole fractions were measured. The peak areas were matched with the vapour mole fractions predicted by the PRSV equation. This calibration curve (Figure 4.2) was used to convert experimental peak areas to a vapour mole fraction.

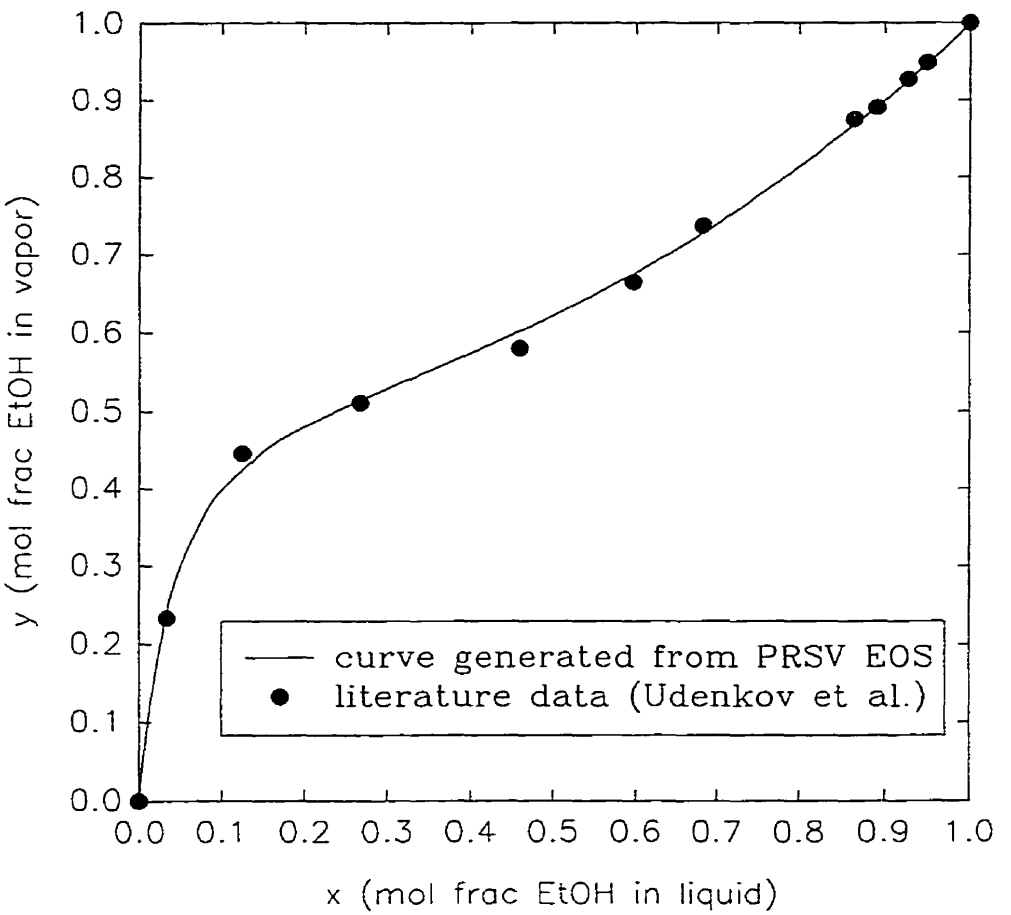

Figure 4.1: Comparison of vapour-liquid equilibrium data from PRSV equation of state and published data (Udenkov et al., 1952) for ethanol/water system at 60°C.

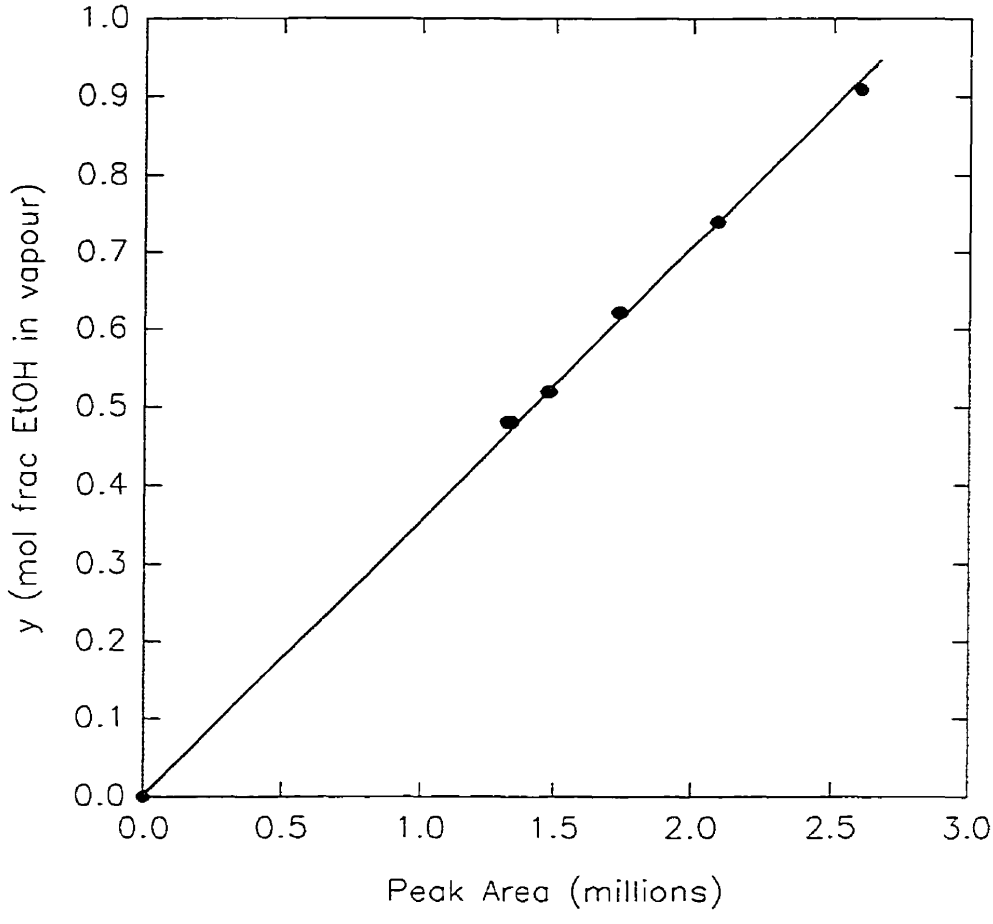

Figure 4.2: Calibration curve for conversion of experimental peak areas to vapour mole fractions of ethanol.

Similarly, the published data of Schrfiber *et al.* (1976) was used for peak area conversions for the 1-propanol/water system at 60°C. Figure 4.3 is the calibration curve used for conversion of data.

4.3 Reproducibility of Data

The use of the autosampler greatly reduced variations in data. The standard deviation of vapour mole fraction without interface modification was less than 1.5% with three replicates at each liquid mole fraction measured. The standard deviation of results from vials equipped with capillary plates was less than 2%. This was slightly larger due to the liquid level adjustments required for each run.

4.4 Effects of Liquid Volume

To study the effects of liquid volume, vials were filled with different volumes of ethanol/water solutions with a liquid mole fraction of 0.3847 and the vapour compositions were measured. The results are summarized in Table 4.1 below.

Table 4.1: Liquid volume and peak area.

liquid volume (ml)	vapour volume (ml)	peak area	y (vapour mole fraction of EtOH)
4	18	1 617 253	0.574
12	10	1 619 488	0.575
15	7	1 618 221	0.574

Volume did not have a significant effect on the vapour composition as long as there was a sufficient volume of liquid to keep the liquid composition from changing. Assuming ideal solutions, the change in ethanol mole fraction of 0.3847 in the liquid was calculated for the system at equilibrium with liquid and vapour volumes of 4ml and 18ml respectively (Appendix C). Since the number of moles of alcohol in the vapour was found to be 0.4% of the moles in the liquid, the liquid mole fractions were deemed to remain constant.

4.5 Liquid above and below plates

A set of experiments was carried out to ensure that neither leaching nor adsorption affected the vapour mole fraction. Three conditions of liquid levels in the vials were studied (Figure 4.4). In case (a), sintered metal plates were placed on the bottom of the vial and the liquid volume was 10ml. In case (b), 7ml of liquid was placed in the vial. The liquid level was approximately 1cm below the plate. The liquid level was 1cm above the plate in case (c) and the liquid volume was 13ml. In case (a), the GC peak area for the bulk solution was 4 564 199 and for the vial with metal plates on the bottom of it was 4 555 059. Results for cases (b) and (c) are shown in Figure 4.5. The peak areas in the vial without plates and the vial with the plates on the bottom did not show any significant difference in the t-test. Similarly, as shown in Figure 4.5, the peak areas for plates with the liquid level above them had no significant differences from the peak areas of the bulk solution. This indicated that the leaching of impurities or adsorption were not factors in the

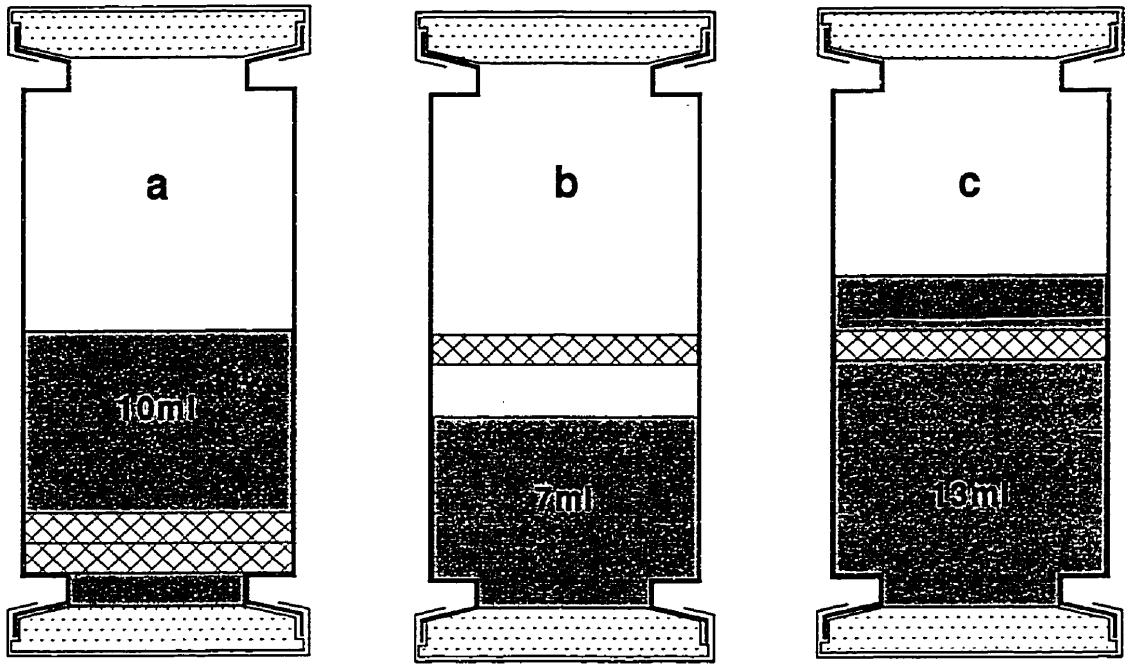

Figure 4.4: Liquid level in sample vials: (a) 10ml of solution with metal plates on bottom of vial, (b) 7ml of solution with liquid level below plate and (c) 13ml of solution with liquid level above plate.

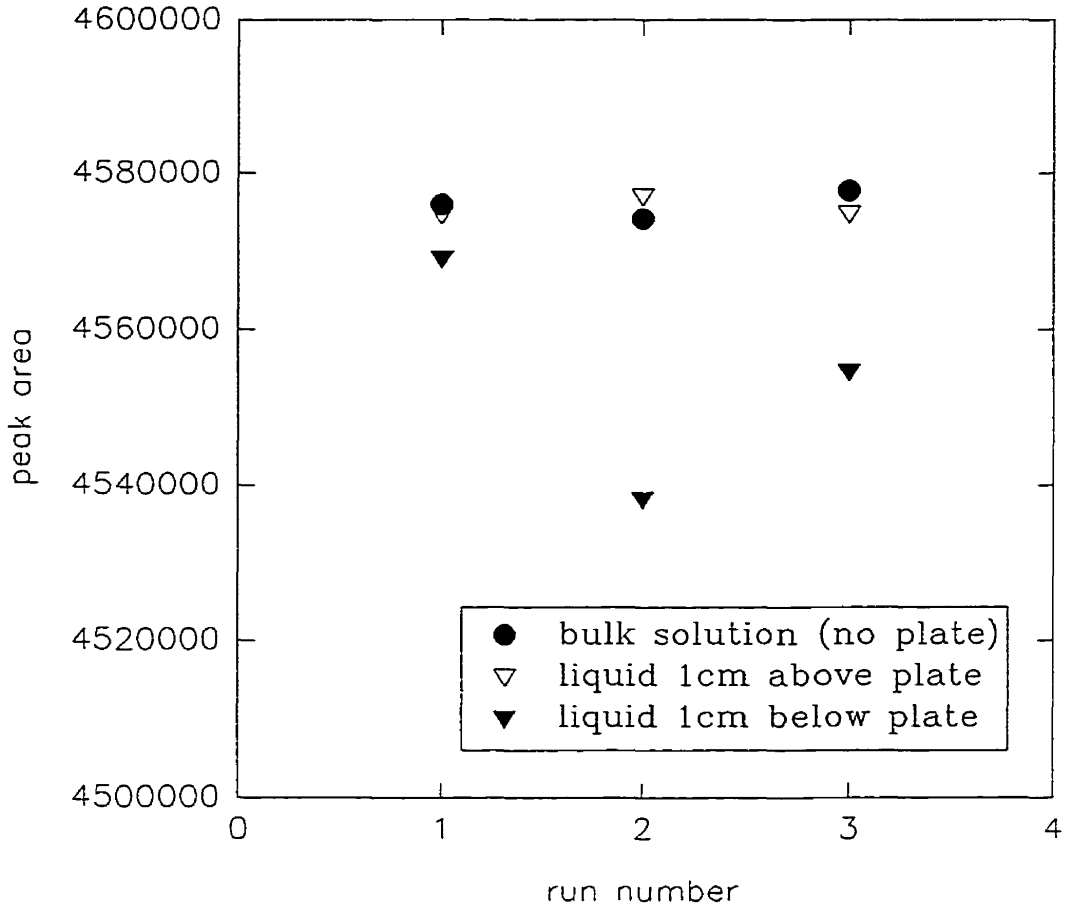

Figure 4.5: Results for experiments with liquid level below and above sintered metal plates for ethanol/water system at x_{EtOH}=0.2 and 60°C.

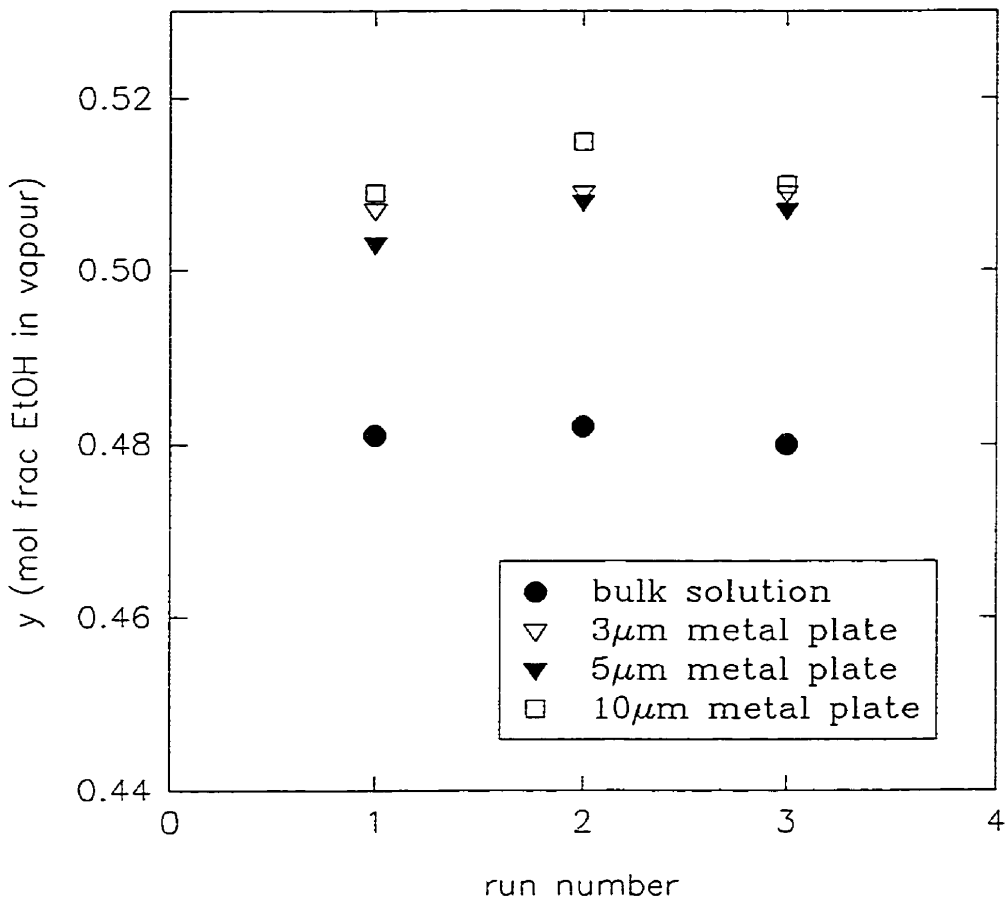

Figure 4.6: Effects of pore sizes on vapour ethanol mole fraction with 3, 5 and 10μm sintered metal plates at x_{EtOH}=0.2 and 60°C.

(a)

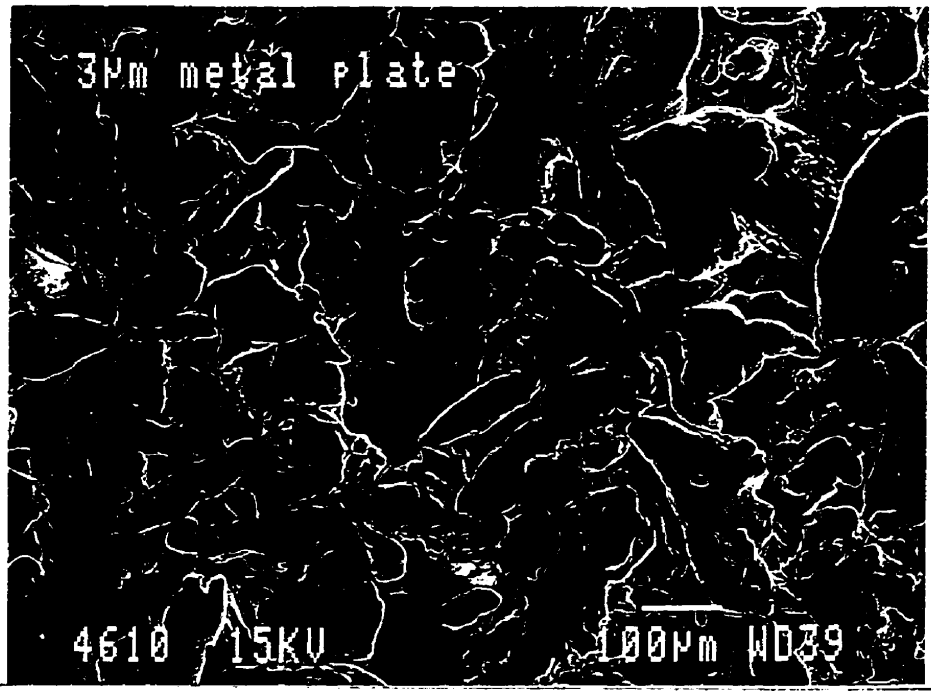
3μm metal plate
4610 15KV
100μm WD39

(b)

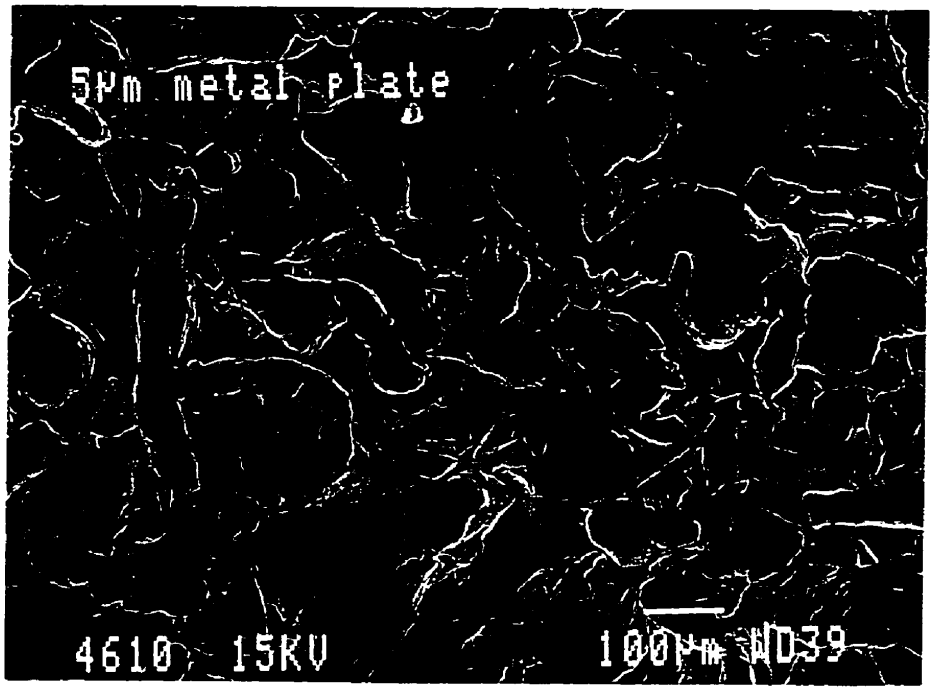
5μm metal plate
4610 15KV
100μm WD39

(c)

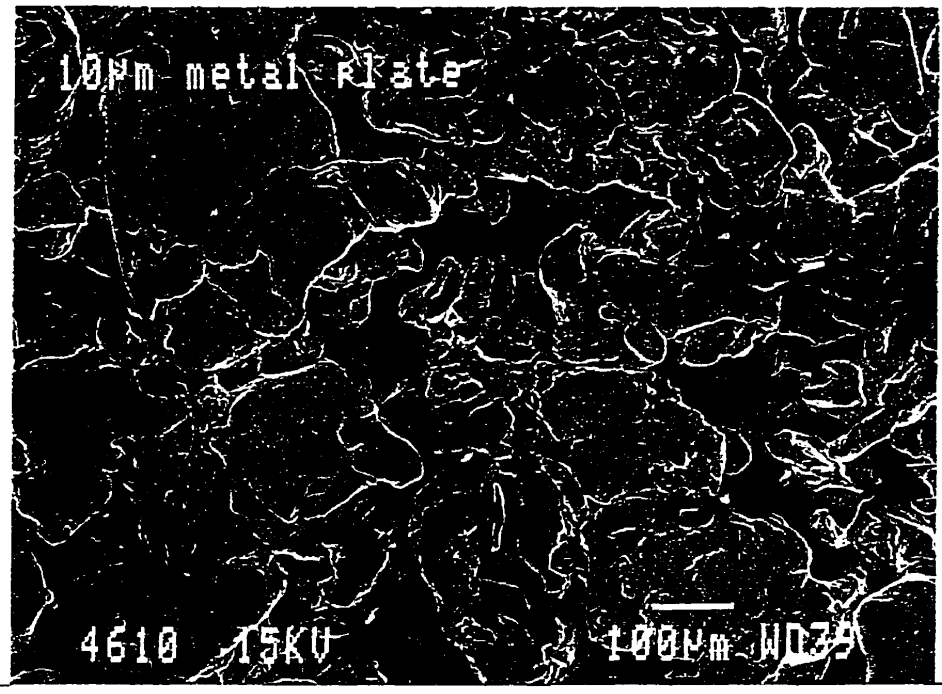

(d)

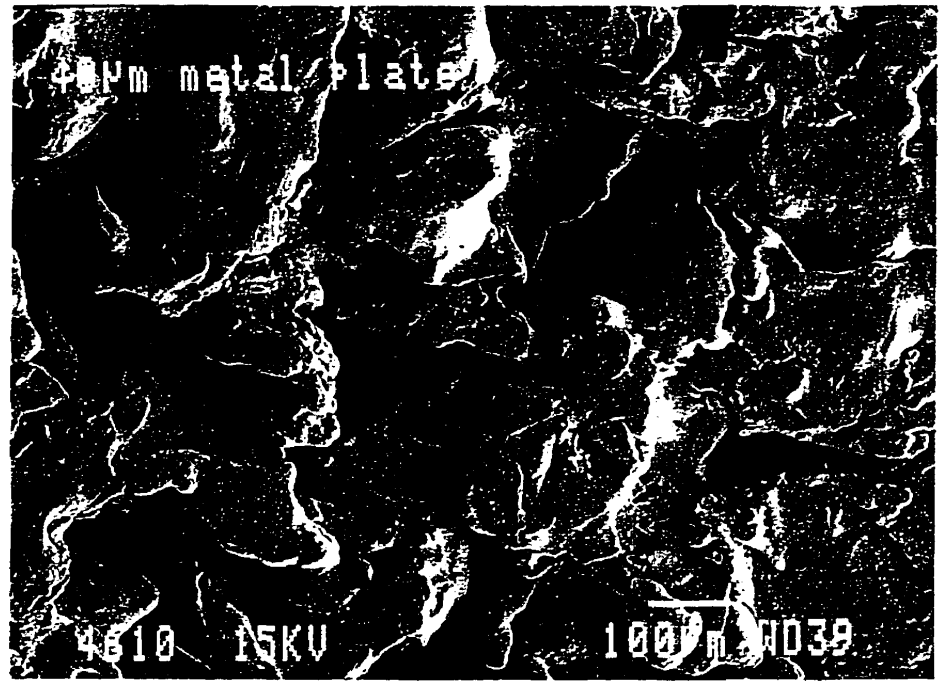

Figure 4.7: SEM photographs of sintered stainless steel plate surfaces: (a) 3µm, (b) 5µm, (c) 10µm and (d) 40µm.

4.6.2 5μm Metal Plate

The ethanol/water system at 60°C was studied with the 5μm plate at liquid mole fractions of 0.2 to 1.0. The results are compared to the PRSV data in Figure 4.8. There are significant differences as tested with the t-test with a confidence interval of 99% all along the range of liquid mole fractions. An interesting point is at the azeotrope. The azeotrope for a solution with planar interface at 60°C is located at a mole fraction of 0.89. At this point in Figure 4.8, the vapour mole fraction with the metal plate was higher than 0.89. Therefore, the azeotrope was moved to a higher concentration. The experimental curve met the generated curve at a liquid concentration of approximately 0.96. This confirmed that the mechanism behind this behaviour could not be solely condensation. Should vapour condense in the plate and the vapour mole fraction be higher as in a distillation column, there would be no difference noted at the azeotropic point.

To predict the shift in azeotrope in a capillary system, the following equation suggested by Defay *et al.* (1966) was used:

$$x_{2,az} - (x_{2,az})_o = -\frac{\sigma}{\partial\sigma/\partial x_2''} \ln\left(1 + \frac{v_1'' - v_2''}{\alpha r} * \frac{\partial\sigma}{\partial x_2''}\right) \qquad (4.2)$$

where in this case, component (1) is water and component (2) is ethanol. σ is the surface tension of the mixture, $(x_{2,az})_o$ is the azeotrope of the system over a planar vapour-liquid interface. v_1'' and v_2'' are the liquid molar volumes of the two components. x_2'' is the ethanol mole fraction in the liquid phase and $x_{2,az}$ is the azeotrope mole fraction in a capillary system. Implicit in the equation are the

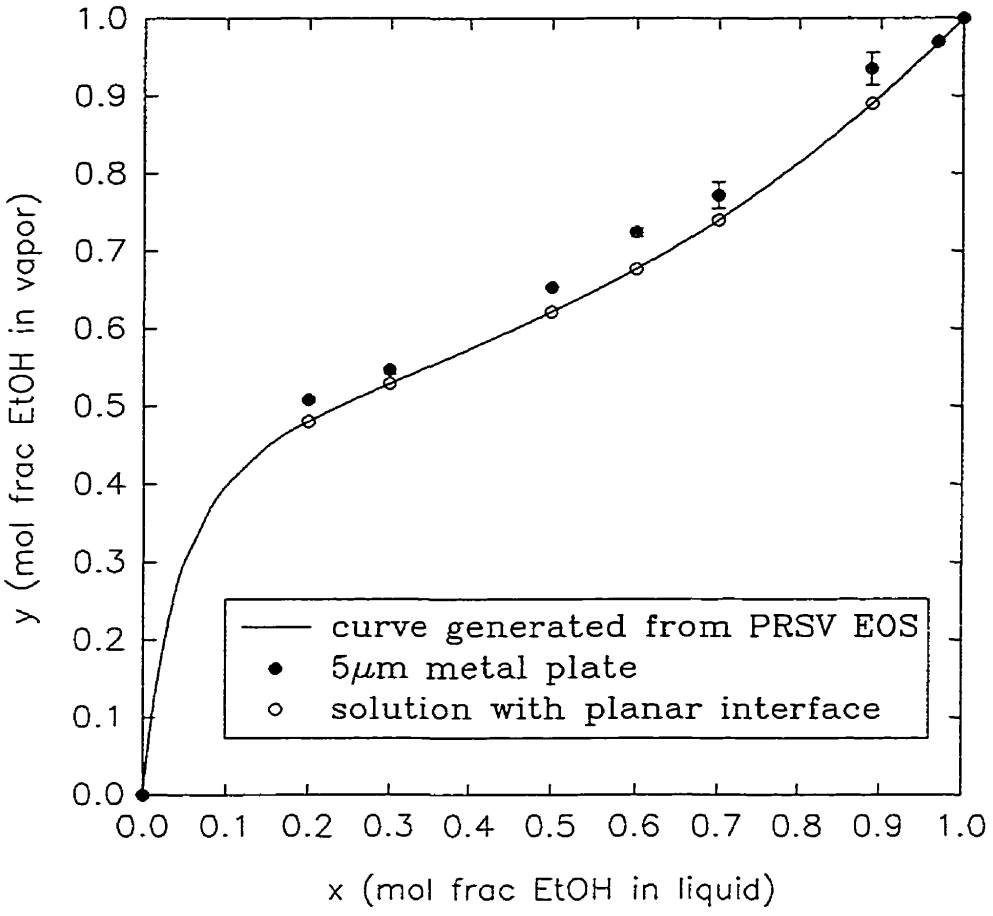

Figure 4.8: Experimental vapour-liquid equilibrium data for ethanol/water system with 5μm sintered metal plate at 60°C.

assumptions that the solutions were ideal and the liquid properties were independent of r, the radius of curvature. Details of the calculations can be found in Appendix C.

Equation 4.2 predicts the azeotrope mole fraction to be at 0.89003. However, experimentally the vapour mole fraction of the system with capillary plates over a liquid mole fraction of 0.89 is above 0.93.

The 5μm plate was also tested with the 1-propanol/water system at 60°C. There were significant differences in vapour mole fractions in the range of liquid mole fractions of 0.2 to 0.8 (Figure 4.9). The azeotropic point for a planar interface system occurs at a mole fraction of 0.43. However, with the sintered plate, the point was again shifted to a higher mole fraction.

A disadvantage of using metal plates was that rust developed on the plates after 6 months of use. SEM results indicated no change in pore shapes or sizes at the rusting sites. Replicates of concentrations tested early in the experimental sequence indicates that the presence of rust did not change the results.

4.6.3 Glass plates

Runs at conditions similar to the metal plate were performed on the fine (4-8μm) and medium (10-20μm) glass plates. Unlike the metal plates, the liquid wetted the glass plate more easily, even at low alcohol concentrations.

The results of the fine glass plates are plotted in Figure 4.10. The vapour mole fractions were significantly higher than those of the bulk solutions. Again, the

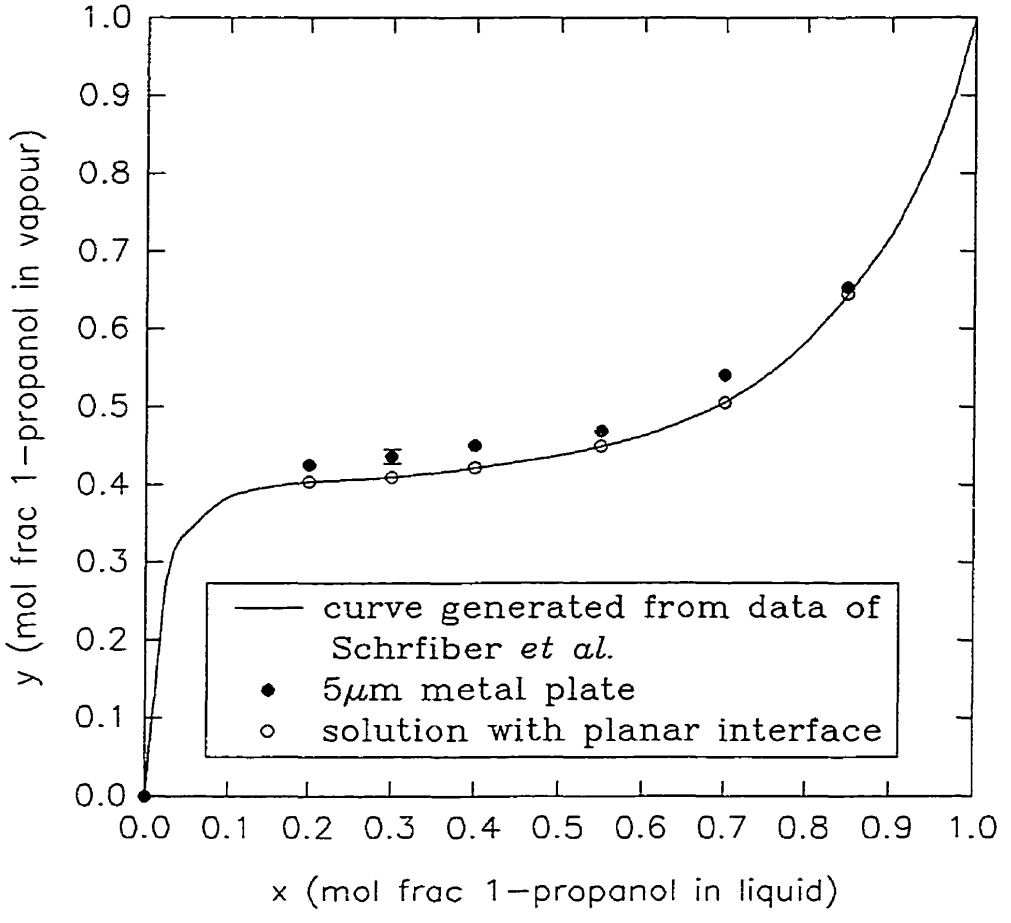

Figure 4.9: Experimental vapour-liquid equilibrium data for 1-propanol/water system with 5μm sintered metal plate at 60°C.

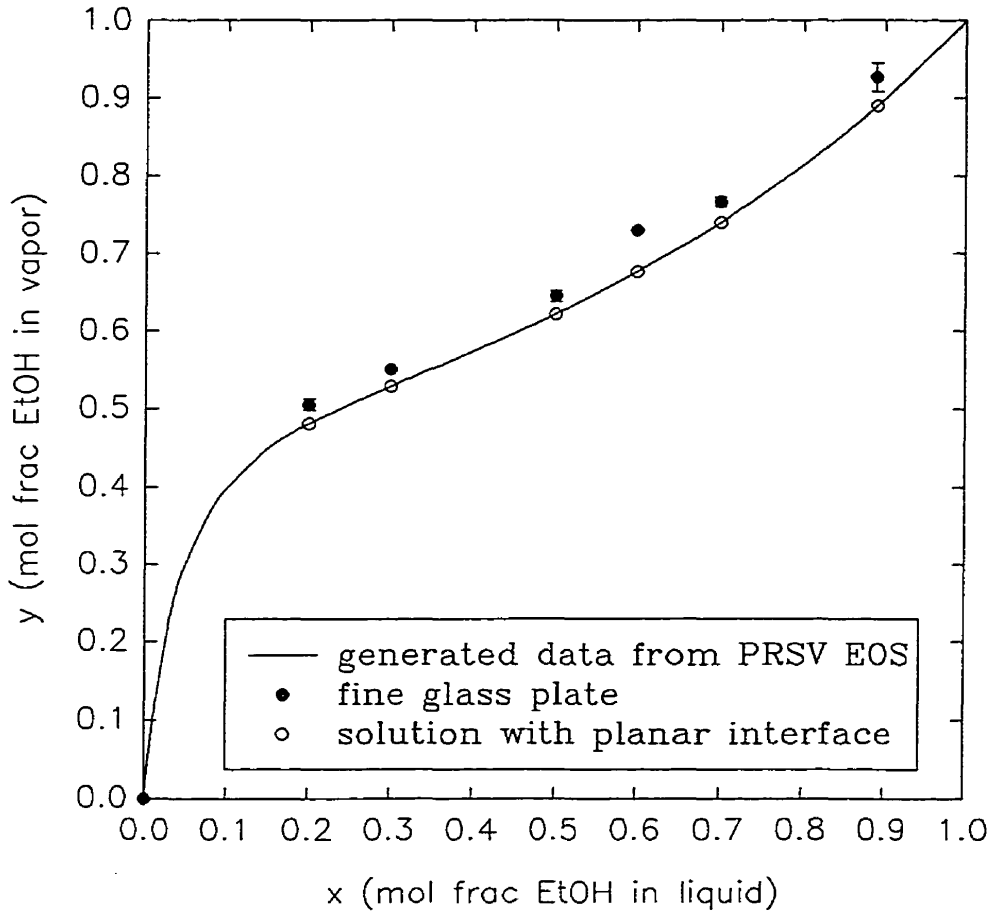

Figure 4.10: Experimental vapour-liquid equilibrium data for ethanol/water system with fine fritted glass plate (4-8μm) at 60°C.

azeotrope was moved to a higher mole fraction from 0.89. Similar results were obtained with the 1-propanol/water system (Figure 4.11). The t-test with a confidence interval of 99% was used for all the data.

On the other hand, the medium glass plate did not have any effect on the vapour mole fraction throughout the range of liquid mole fractions (Figure 4.12). For comparison, a vial modified with a 40μm metal plate was also studied under the same conditions. Even though the nominal metal pore size was twice as large as the medium glass plate, it increased the vapour mole fractions (Figure 4.13). Several factors were considered. The contact angles and radii of curvature would be different for steel and glass. Since the glass plates were wetted more easily than the metal plates, the interface may have a larger curvature (smaller effect). A second factor would be the shape of the pores on the plates. The SEM photographs in Figure 4.14 show that the fine glass plates are composed of spherical beads with a mean pore diameter of 27±9μm. The medium glass plates are made from randomly compacted elongated glass rods with a pore diameter of 34±10μm. The shape of the pores are more irregular in the medium glass plate which may affect the radius of curvature of the pores.

4.7 Membrane

The Durapore polyvinylidene fluoride membrane with a pore size of 0.45μm was chosen because of its hydrophobic properties and its resistance to alcohols. The membrane swelled at high concentrations of alcohol but did not break down.

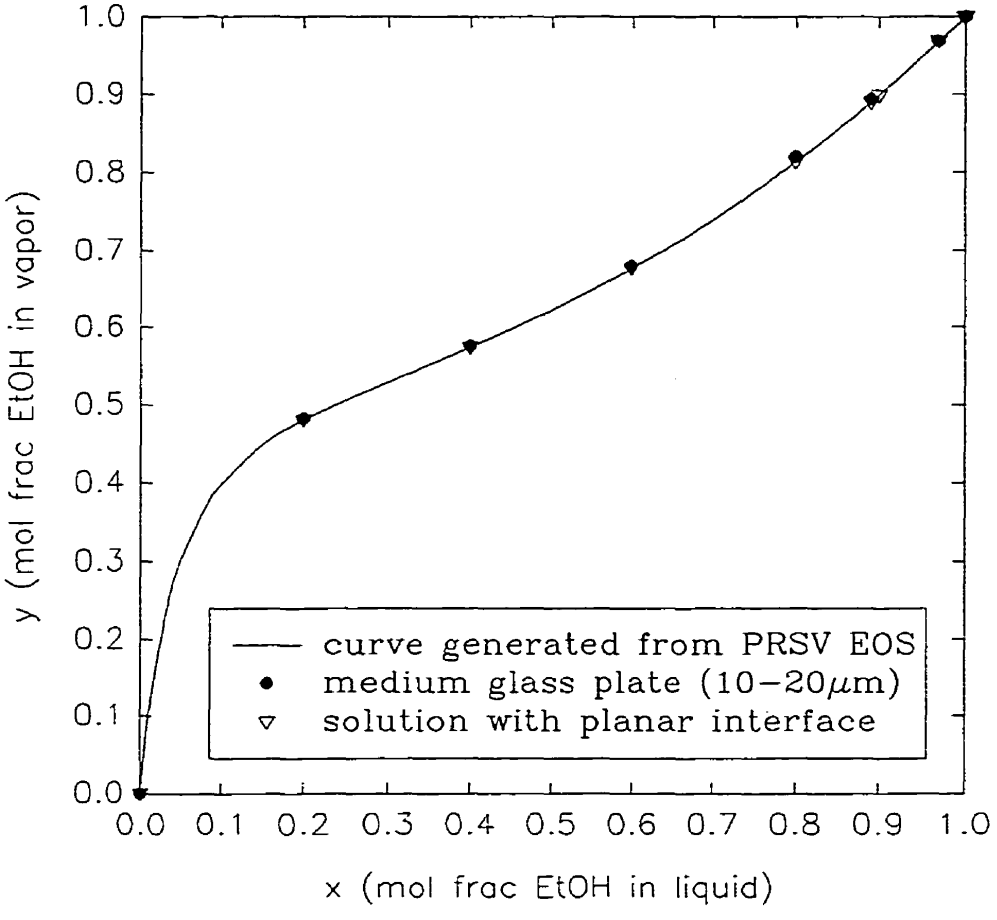

Figure 4.12: Experimental vapour-liquid equilibrium data for ethanol/water system with medium fritted glass plate (10-20μm) at 60°C.

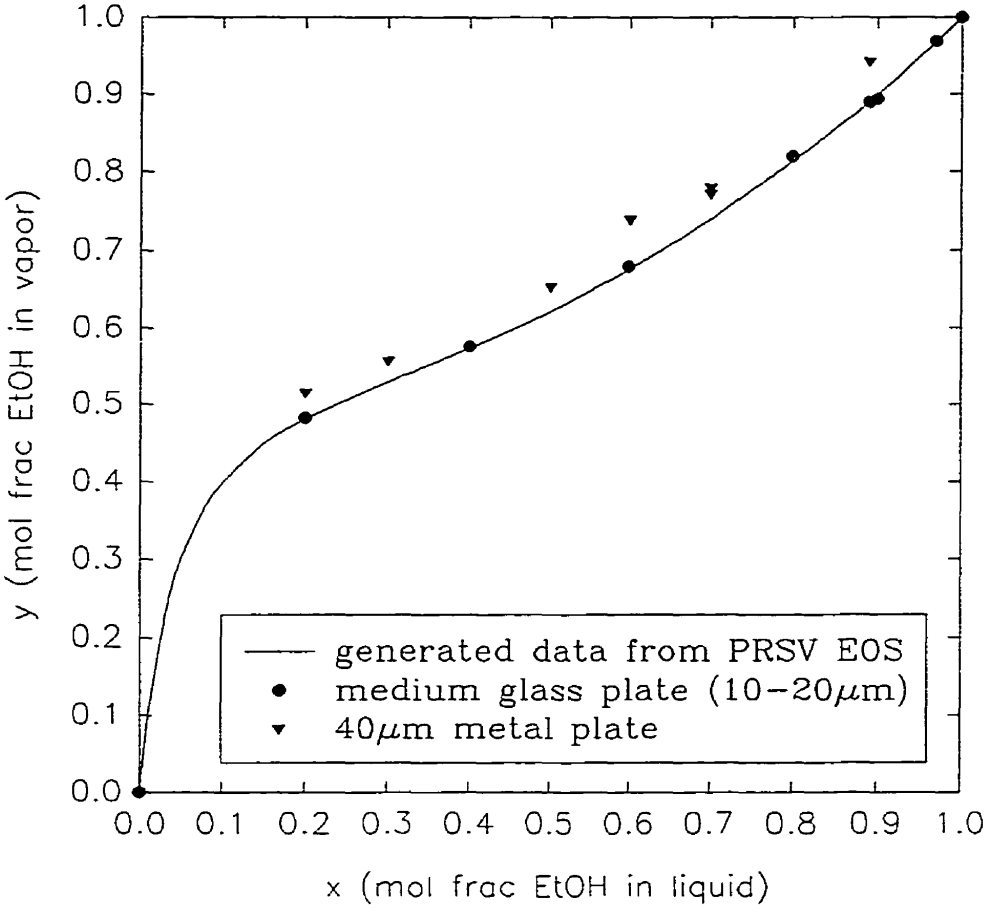

Figure 4.13: Comparison of medium glass plate (10-20μm) and 40μm metal plate vapour-liquid equilibrium data for ethanol/water system at 60°C.

(a)

(b)

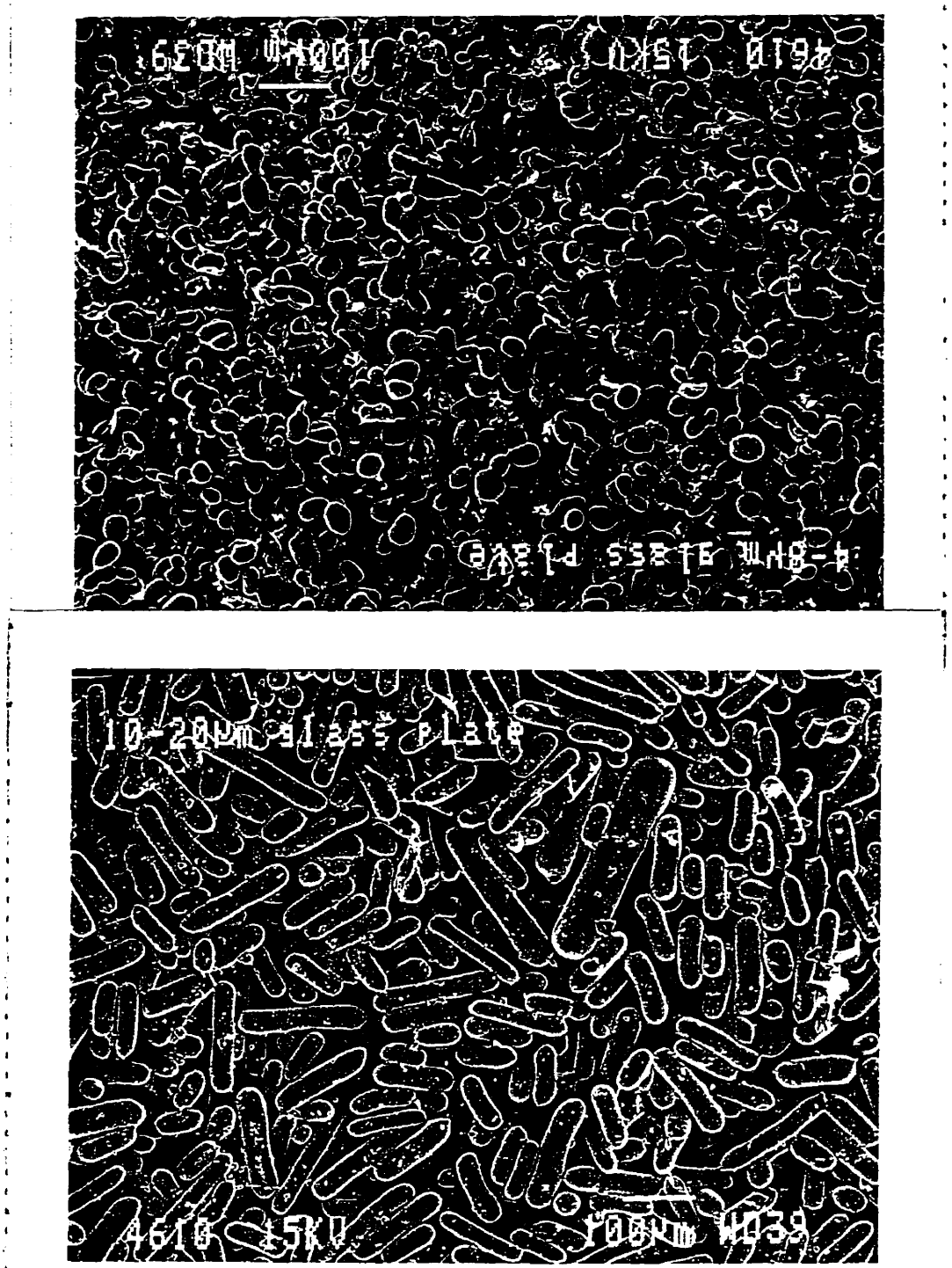

Figure 4.14: SEM photographs of fritted glass plate surfaces: (a) fine (4-8μm) and (b) medium (10-20μm).

As discussed in Chapter 3, section 3.2, the membrane was supported on a stainless steel perforated plate. A vial with the perforated plate alone was filled with a 0.4 mole fraction ethanol solution and the peak area was compared with that of the bulk solution. The peak area of 4 987 678 for the perforated plate was not significantly different from the bulk solution peak areas of 5 000 328 and 4 999 225. The t-ratio with a confidence interval of 99% was used to test the data. The membrane support was thus eliminated as a possible contributing factor.

The effects of the membrane can be seen in Figure 4.15 for the ethanol/water system and Figure 4.16 for the 1-propanol/water system. Results were similar to those of the metal and fine glass plates.

The structure of the membrane was studied under the SEM and the mean pore diameter was found to be 1.3±0.6μm (Figure 4.17). The pores have a smaller distribution in size and the shapes are much more circular than the other plates.

To test the extreme effect of pore size distribution, a hole approximately 5% in area of the total membrane area was made. The peak area of 1 877 629 was not significantly different from the bulk peak area of 1 872 327. Therefore, a large pore on the membrane would cancel out the effects of the smaller pores.

4.8 Kelvin Equation Prediction

As seen in section 4.6.1, there was a 6-9% increase in vapour mole fraction when the interface was modified with the sintered metal plate at a liquid ethanol mole fraction of 0.2. Using the Kelvin equation for a mixture in capillary systems

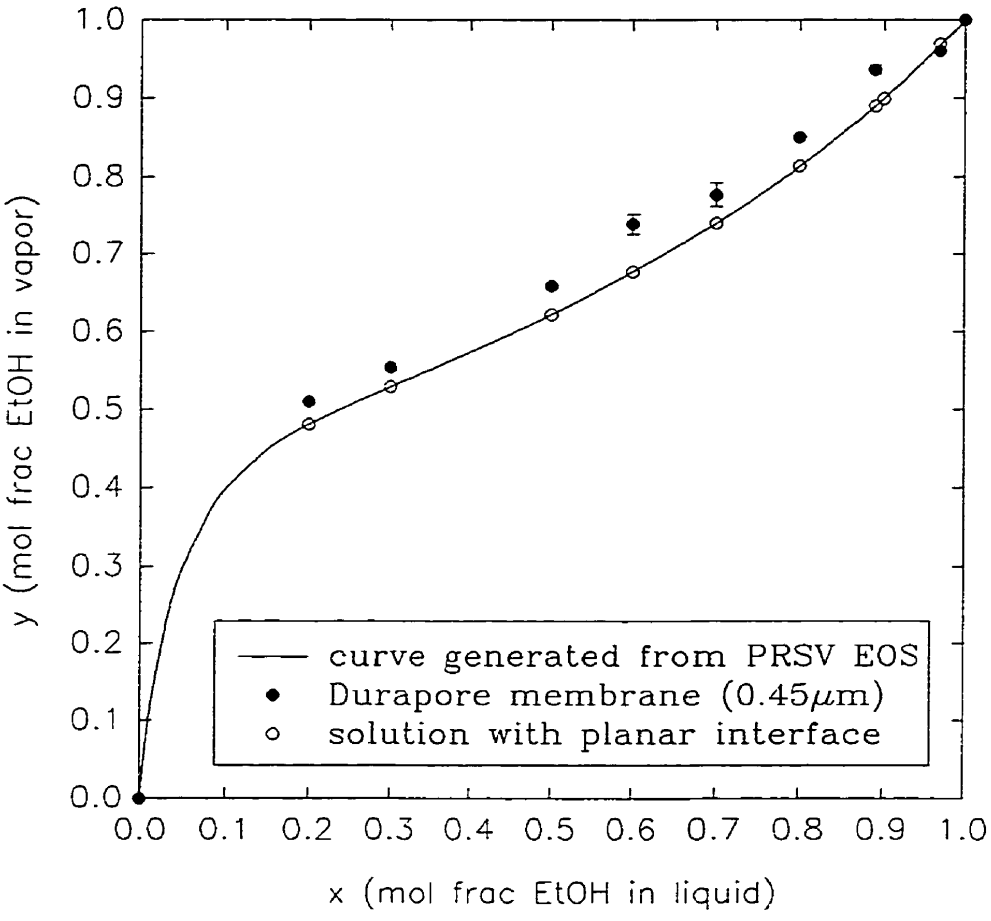

Figure 4.15: Durapore membrane (0.45μm) vapour-liquid equilibrium data for ethanol/water system at 60°C.

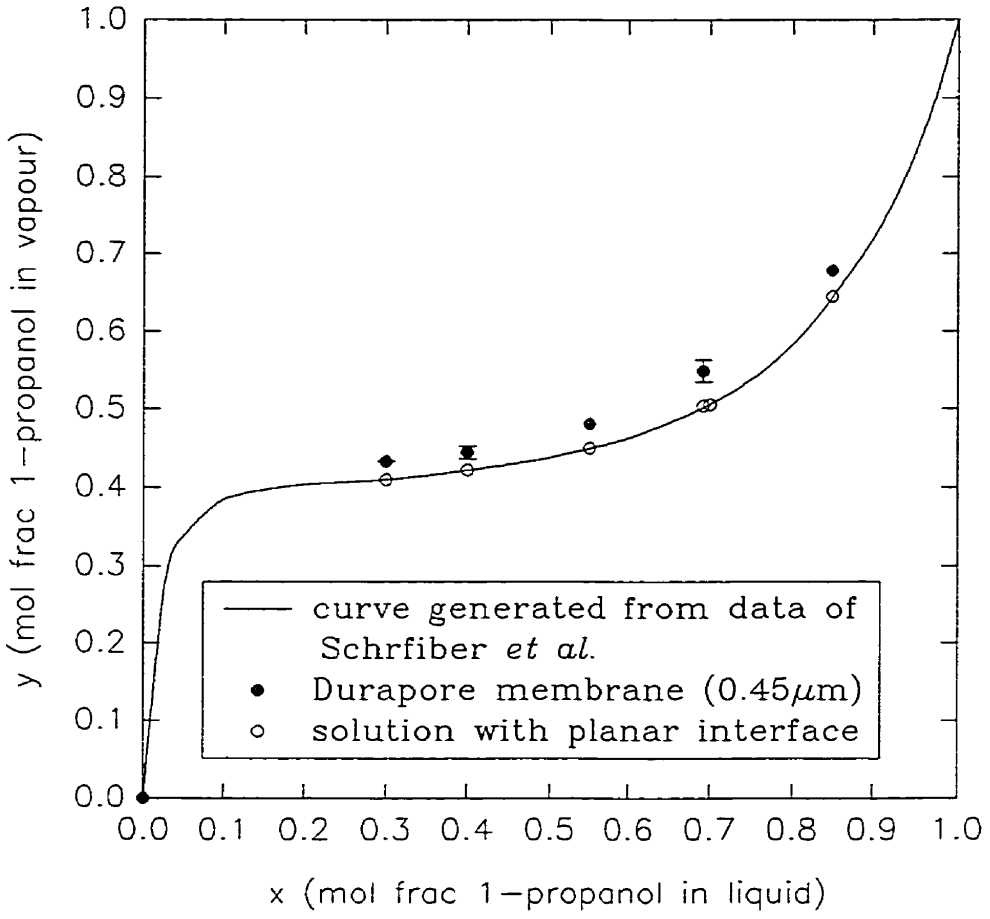

Figure 4.16: Durapore membrane (0.45μm) vapour-liquid equilibrium data for 1-propanol/water system at 60°C.

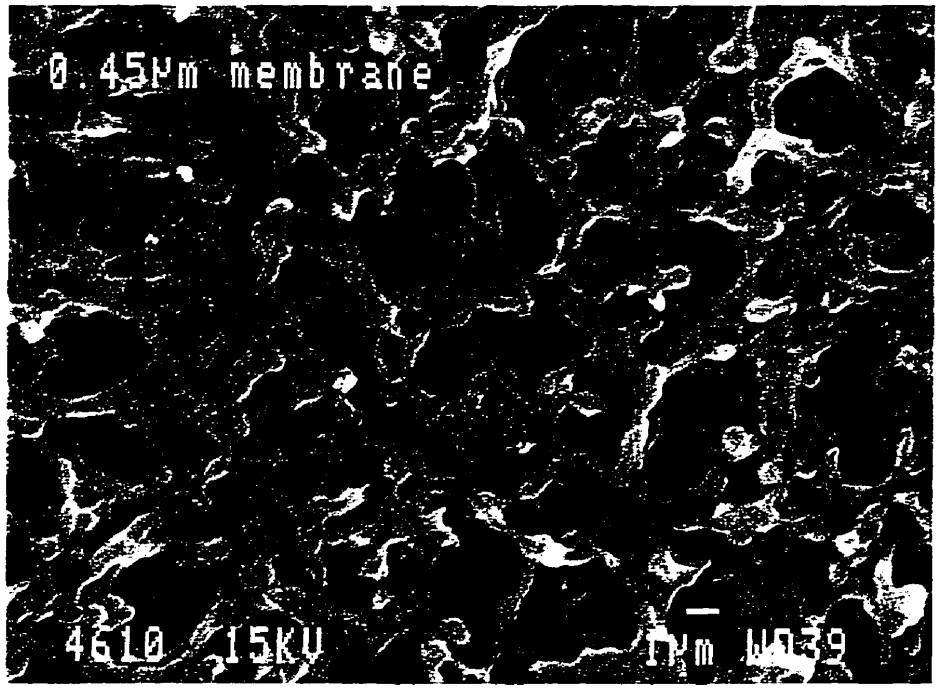

Figure 4.17: SEM photograph of Durapore membrane (0.45µm) surface.

(equation 4.3),

$$\ln \frac{p}{p^o} = -\frac{2\,\sigma\,v}{r_{pore}\cos\theta\;R\;T} \qquad (4.3)$$

the pore radius r_{pore} required to obtain a vapour mole fraction difference of 6% was calculated (Appendix C). It was assumed that the vapour was an ideal gas so that pressures p and p° were directly proportional to vapour mole fractions y and y°. The superscript ° refers to the property over a plane liquid interface. The pores were assumed to be cylindrical and the meniscus to be hemispherical so that the radius of curvature r was equal to the contact angle θ multiplied by r_{pore}. The results are summarized in Table 4.3. The pore size predicted by the Kelvin equation is two orders of magnitude smaller than those on the actual sintered plates used.

Table 4.3: Comparison of experimental results and Kelvin equation prediction.

	Pore Size	y_{EtOH} increase over bulk sol^n
experimental	3-10μm	6%
Kelvin equation	3-10μm	0%
Kelvin equation	0.012μm	6%

4.9 Comparison to Literature Data

Yeh *et al.* (1986) studied the vapour-liquid equilibrium of ethanol/water

system at 50°C using an isothermal static method. The capillary plates used were stainless steel sintered plates. The authors found a difference of 25% in vapour mole fraction between the bulk phase and the modified system at a liquid mole fraction of 0.2 ethanol. They attributed this difference to three main forces: (1) the London force dispersion interactions; (2) induction force polar interactions; and (3) the radius of curvature effects. Yeh *et al.* suggested that the Kelvin equation only predicted the effect of curvature but did not take into account the other forces that are present in a polar solution.

Since the size and shape of the pores will affect these interactions, the variation in results between this thesis and that of Yeh *et al.* may be due to the different plates used.

4.10 Summary

Stainless steel sintered metal plates(3-40μm), fine fritted glass plate (4-8μm) and the Durapore membrane (0.45μm) affected the VLE of the ethanol/water and 1-propanol/water systems. The increase in the alcohol vapour mole fraction is much greater than the values predicted by the Kelvin equation. The pore size predicted by the Kelvin equation that is required to produce the same difference in ethanol vapour composition as observed experimentally is two orders of magnitude smaller than the plates tested. The shift in azeotrope predicted by Defay is from 0.89 to 0.89003. However, experimentally, the vapour mole fraction at a liquid mole fraction

of 0.89 is approximately 0.93. The material of the capillary system, the pore size and the shape of the pores all play a role in the degree of the effect. Table 4.4 summarizes the results of the different plates and the figures in which they appear in the chapter.

Table 4.4: Summary of results and figures.

Capillary Plate		Ethanol/Water System	1-Propanol/Water System
sintered metal plates	3μm	- increase of 6-9% in ethanol vapour mole fraction at ethanol liquid mole fraction of 0.2 - shift in azeotrope **(Fig. 4.6 and 4.8)**	--
	5μm		- increase in propanol vapour mole fraction - shift in azeotrope **(Fig. 4.9)**
	10μm		--
	40μm	- increase in ethanol vapour mole fraction - shift in azeotrope **(Fig. 4.13)**	--
fritted glass plates	fine (4-8μm)	- increase in ethanol vapour mole fraction - shift in azeotrope **(Fig. 4.10)**	- increase in propanol vapour mole fraction - shift in azeotrope **(Fig. 4.11)**
	medium (10-20μm)	- no effect on ethanol vapour mole fraction **(Fig. 4.12)**	--
Durapore membrane (0.45μm)		- increase in ethanol vapour mole fraction - shift in azeotrope **(Fig. 4.15)**	- increase in propanol vapour mole fraction - shift in azeotrope **(Fig. 4.16)**

5.0 CONCLUSIONS AND RECOMMENDATIONS

5.1 Conclusions

Vapour-liquid interface modifications in ethanol/water and 1-propanol/water systems with sintered metal plates, fritted glass plates and membrane were tested. The conclusions of the experiments are summarized below:

- An experimental vessel for the capillary plates was designed to use with the gas chromatograph autosampler.

- The GC and autosampler parameters that gave the most reproducible results were determined and used for all experiments. A calibration method was developed to convert GC peak areas to vapour mole fractions of alcohol.

- Leaching, adsorption and condensation were eliminated as significant factors in the increase of the vapour mole fraction.

- Sintered metal plates of nominal pore sizes between 3-40μm, fine fritted glass plates (4-8μm) and 0.45μm Durapore membrane all significantly increased the vapour mole fraction above that of bulk solutions. The pore size predicted by the Kelvin equation that was required to cause a 6-9% increase was 2 orders of magnitude smaller than the nominal pore size experimentally used.

- There was a shift in the azeotrope composition for both the ethanol/water and 1-propanol/water systems that was much greater than predicted theoretically.

- Scanning electron microscope images indicate that the pores on the surface of the plates are non-circular and the pores are much larger than the nominal pore size stated.

- The shape of the pore is an important factor. This was observed for the fine glass plate and the medium glass plate. The fine glass plate which caused an increase in vapour mole fraction was composed of glass spheres. However, the medium glass plate made up of glass rods did not affect the vapour mole fraction.

5.2 Recommendations

- Since the shape of the pores affects the radius of curvature, a porous medium with uniform cylindrical pores may have a larger effect on the vapour mole fraction and should be tested.

- By preheating the liquid or adding a side outlet to the housing, the liquid level may be controlled more precisely.

- Other aqueous organic systems with azeotropes should be tested to see whether the azeotrope composition will be shifted with capillary plates.

- Test binary systems where both components can be detected by the GC so that the vapour mole fractions can be directly determined.

- Instead of just one capillary plate, use a stack of plates to simulate a column.

- If the vapour sample is directly injected into the GC, the housing will not be dimensionally constrained by the autosampler and a larger capillary plate surface area could be tested.

REFERENCES

Boucher, E.A., "Capillary Phenomena", J. Chem. Soc., Faraday Trans. 1, 80 (1984) 3295-3305.

Boucher, E.A., "Vapour Pressure Over Free and Capillary-Condensed Curved Surfaces of Aqueous Salt Solutions and of Non-Electrolyte Solutions", Colloids and Surfaces, 46 (1990) 271-281.

Coleburn, N.L., and Shereshefsky, J.L., "Liquid-Vapour Equilibrium in Microscopic Capillaries", J. of Colloid and Interface Science, 38 (1972) 84-90.

Defay, R., Prigogine, I., Bellemans, A. and Everett, D.H., Surface Tension and Adsorption, John Wiley and Sons, New York, 1966.

Gmehling, J. and Onken, U. Vapor-Liquid Equilibrium Data Collection, Dechema, Deutsche Gesellschaft fur Chemisches Apparatewesen, 1981.

Kuz, V.A., "Thermodynamic vapour pressure equation. Triple and critical point applications. Prediction of a linear logarithmic relation between surface tension and latent heat of evaporation", Fluid Phase Equilibria, 66 (1991) 113-124.

Li, D. and Neumann, A.W., "Equilibrium of Capillary Systems with an Elastic Liquid-Vapour Interface", Langmuir, 9 (1993) 50-54.

Li, D., "Curvature Effects on the Phase Rule", Fluid Phase Equilibria, 98 (1994) 13-34.

Marsh, K.N., "New Methods for Vapour-Liquid-Equilibria Measurements", Fluid Phase Equilibria, 52 (1989) 169-184.

Panagiotopoulos, A.Z., "Adsorption and capillary condensation of fluids in cylindrical pores by Monte Carlo simulation in the Gibbs ensemble", Molecular Physics, 62 (1987) 701-719.

Perry, R.H., ed., Perry's Chemical Engineers' Handbook, 6th ed. McGraw Hill Book Company, 1984.

Prigogine, I. and Defay, R., Chemical Thermodynamics, Longmans, 1954.

Sperry, David P., Falconer, John L. and Noble, Richard D., "Methanol-hydrogen separation by capillary condensation in inorganic membranes", Journal of Membrane Science, 60 (1991) 185-193.

Stryjek, R. and Vera, J.H. "PRSV: An Improved Peng-Robinson Equation of State for Pure Compounds and Mixtures", The Canadian Journal of Chemical Engineering, 64 (1986) 323-333.

Stryjek, R. and Vera, J.H. "PRSV: An Improved Peng-Robinson Equation of State with New Mixing Rules for Strongly Nonideal Mixture", The Canadian Journal of Chemical Engineering, 64 (1986) 334-340.

Stryjek, R. and Vera, J.H. "PRSV2: A Cubic Equation of State for Accurate Vapor-Liquid Equilibria Calculations", The Canadian Journal of Chemical Engineering, 64 (1986) 820-826.

Troung, J. and Wayner Jr., P.C., "Effects of capillary and van der Waals dispersion forces on the equilibrium profile of a wetting liquid: Theory and experiment", J. Chem. Phys, 87 (1987) 4180-4188.

Wankat, P., Equilibrium Staged Separations, Prentice Hall, Inc., New Jersey, 1988.

Yeh, G.C., Shah, M.S. and Yeh, B.V., "Vapour-Liquid Equilibria of Nonelectrolyte Solutions in Small Capillaries. 1. Experimental Determination of Equilibrium Compositions", Langmuir, 2 (1986) 90-96.

Yeh, G.C., Yeh, B.V., Ratigan, B.J., Correnti, S.J., Yeh, M.S., Pitakowski, D.W., Fleming, W., Ritz, D.B. and Lariviere, J.A., "Separation of Liquid Mixtures by Capillary Distillation", Desalination, 81 (1991a) 129-160.

Yeh, G.C., Yeh, B.V., Schmidt, S.T., Yeh, M.S., McCarthy, A.M. and Celenza, W.J., "Vapour-Liquid Equilibrium in Capillary Distillation", Desalination, 81 (1991b) 161-187.

NOMENCLATURE

[P] = dependent on structure of molecule

σ_{mix} = surface tension of mixture (dynes/cm)

σ_w = surface tension of pure H_2O (dynes/cm)

σ_e = surface tension of pure EtOH (dynes/cm)

x = bulk liquid mole fraction

v = molar volume of pure components (cm^3/mol)

q = parameter dependent on mixture (q=2 for polar mixture)

ρ = density (mol/cm^3)

p = pressure

θ = contact angle

r = radius of curvature

r_{pore} = radius of pore

R = gas constant

T = temperature of system

subscripts

w = water

e = ethanol

l = liquid phase

g = gas phase

o = bulk phase

APPENDIX A

PROCEDURE FOR HEADSPACE AUTOSAMPLER

1. Sample vials are placed on the 50-position carrousel.
2. Program parameters in one of four methods (4 methods can run consecutively by using "schedule" set-up).
3. Vial is automatically loaded into the 12-position platen to be heated to the preset temperature.
4. Vial is raised onto the needle after the sample equilibrium time has been reached.
5. The pressurization gas flows through the needle and pressurizes the vial until the vial pressure has been attained.
6. The gas flow is shut and the vial is allowed to equilibrate.
7. The sample loop is then opened and due to the pressure difference, the sample is forced through and fills the loop.
8. The sample equilibrates in the loop and then travels to the GC carried by the carrier gas.

GAS CHROMATOGRAPH

Column Temperature

The column temperature is set at five degrees above the platen temperature to prevent any condensation in the column.

Setting GC Gas Flow Rates

carrier gas flow rate from headspace (He):	15 cc/min
make-up gas flow rate (He):	15 cc/min
H_2 flow rate:	30 cc/min
Air flow rate:	300 cc/min
Total gas flow rate measured at exit of GC	360 cc/min

APPENDIX B

% initial parameter values

```
Sold=0
S=0
M=10
Pold=0
P1=0
```

% loop to fine pressure of system at EtOH mol frac. x

```
while M>0.001,

    % find molar volume from PRSV eq. of state
    k1=2
    k2=-1

    C1=(k1-1)*b-(R*T/P)
    C2=(k2-k1)*b^2-R*T/P*k1*b+a/P
    C3=-b*(k2*b^2+R*T/P*k2*b+a/P)

    p=C1/3
    q=C2/3
    r=C3/2

    D=q - p^2
    beta=p^3 - 3/2*p*q + r
    E=acos(-beta/sqrt(-D^3))

    V1=2*sqrt(-D)*cos(E/3)-p
    V2=2*sqrt(-D)*cos(E/3+2/3*pi)-p
    V3=2*sqrt(-D)*cos(E/3+4/3*pi)-p

    V(1,1)=V1
    V(2,1)=V2
    V(3,1)=V3

    vv=max(V)
    vl=min(V)

    % calculation of liquid fugacity
    phi_l=fug(P,vl,x)

    % initial vapour fugacity calculation
    phi_v=ifug(P)
```

```
S=2
N=1
Sold=S
% inner loop to converge EtOH vapor mol frac. y

        while N>0.001,

                Stemp=S
                y=x .*phi_l ./phi_v
                S=y(1,1)+y(1,2)
                y=y ./S
                phi_v=fug(P,vv,y)
                N=abs(Stemp-S)
        end

Pold=P1
P1=P
P=P1+(P1+Pold)/(S-Sold)*(1-S)
M=abs(S-1)

end
```

APPENDIX C

Calculation of Change in Liquid Mole Fraction

volume of liquid = 4ml

volume of vapour = 18ml

Iteration #1

x_o = 0.3847

y_o = 0.5704 (PRSV equation of state)

vv = 0.0683 m^3/mol (generated from PRSV equation of state)

vl = 3.8214E-05 m^3/mol (generated from PRSV equation of state)

Initial liquid: = 1.0467 total moles

= 0.4027 moles EtOH

= 0.6441 moles H_2O

In vapour: = 2.6354E-03 total moles of gas

= 1.5033E-03 moles EtOH

= 1.1322E-03 moles H_2O

Moles of ethanol left in liquid = initial moles EtOH - moles EtOH in vapour

= 0.4012 moles EtOH

= 0.6426 moles H_2O

x_1 = 0.3844

Interation #2

x_1 = 0.3844

y_1 = 0.5703 (PRSV equation of state)

vv = 0.0683 m^3/mol (generated from PRSV equation of state)

vl = 3.8201E-05 m^3/mol (generated from PRSV equation of state)

Initial liquid: = 1.0442 total moles

= 0.4012 moles EtOH

= 0.6430 moles H_2O

In vapour: = 2.6354E-03 total moles of gas

= 1.5030E-03 moles EtOH

= 1.1324E-03 moles H_2O

Moles of ethanol left in liquid = initial moles EtOH - moles EtOH in vapour

= 0.4012 moles EtOH

= 0.6430 moles H_2O

x_1 = 0.3842

Change in liquid mole fraction = 0.3%

Therefore, liquid composition assumed to remain constant.

Calculation of surface tension σ for pure compounds @ 60°C (Perry's Handbook)

$$\sigma_w^{1/4} = [P](\rho_l - \rho_g)$$
$$\text{since } \rho_l > \rho_g, \rho_g \to 0$$
$$\sigma_w^{1/4} = [P]\rho_l$$

1. pure H_2O

ρ_l (333.15°C) = 0.054576 mol/cm^3 (Perry's Handbook)

[P] = 51

σ_w = 60.019 dynes/cm

2. pure EtOH

ρ_l (333.15°C) = 0.016575 mol/cm^3 (Perry's Handbook)

[P] = 125.3

σ_w = 18.605 dynes/cm

Calculation of Surface Tension σ for Polar Mixtures (Perry's p.3-288)

$$\sigma_{mix}^{1/4} = \psi_w \sigma_w^{1/4} + (1-\psi_w)\sigma_e^{1/4}$$

$$\log_{10}\frac{(\psi_w)^q}{(1-\psi_w)} = \log_{10}\left[\frac{(x_w V_w)^q}{x_e V_e}(x_w V_w + x_e V_e)^{1-q}\right] + \frac{0.441q}{T}\left[\frac{\sigma_e V_e^{2/3}}{q} - \sigma_w V_w^{2/3}\right]$$

1. σ_{mix} for x_e = 0.2

ψ_w = 0.2969

σ_{mix} = 27.3384 dyne/cm

2. σ_{mix} for x_e = 0.89

ψ_w = 0.01586

σ_{mix} = 19.01 dyne/cm

Calculation of azeotropic mole fraction in a capillary system (Defay)

$$x_{e,az} - (x_{e,az})_o = -\frac{\sigma_{mix}}{\partial\sigma_{mix}/\partial x_{e,l}} \ln\left(1 + \frac{v_{w,l} - v_{e,l}}{\alpha r} \cdot \frac{\partial\sigma_{mix}}{\partial x_{e,l}}\right)$$

$$\alpha = \alpha_2 RT$$

$$\alpha_2 = \frac{1}{x_{e,l}^2} \ln\left(\frac{p}{p_1^o}\right)$$

σ_{mix} = 19.01 dyne/cm

$(x_{e,az})_o$ = 0.89

$\partial\sigma_{mix}/\partial x_{e,l}$ = -41.41 dyne/cm

$v_{w,l}$ = 18.3231 cm^3/mol

$v_{e,l}$ = 60.3318 cm^3/mol

Assuming hemisherical pores, $r = r_p * \theta$

r_p = 10μm

θ = 30°

p = 47.452 kPa

p_w^o = 19.950 kPa

α calculated to be 30.30E09 erg/mol

$x_{e,az}$ = 0.89003

Calculation with Kelvin Equation

Assuming the pores to be cylindrical, radius of curvature r = r_{pore} cos θ.

$$\ln \frac{p}{p^o} = -\frac{2\sigma v}{r_{pore} \cos\theta RT}$$

Assuming ideal gas, pressure P is indirectly proportional to alcohol vapour mole fraction y.

x = 0.2

p/p_o = 1/1.06

σ = 27.3384 dyne/cm

θ = 30°

vl = 3.0261E-05 m^3/mol

R = 8.314 N m/mol K

T = 333.15 K

r_{pore} = 0.012μm

APPENDIX D

IMAGE EVALUATION TEST TARGET (QA-3)

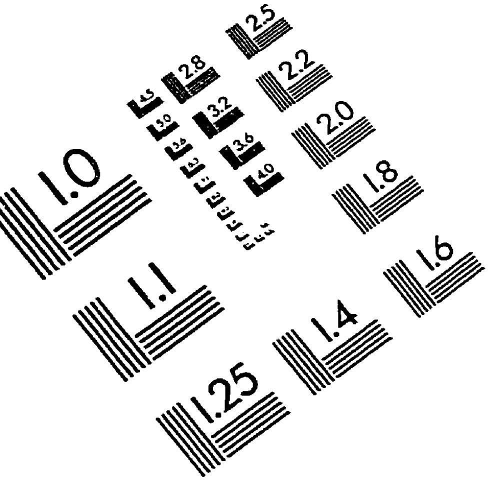

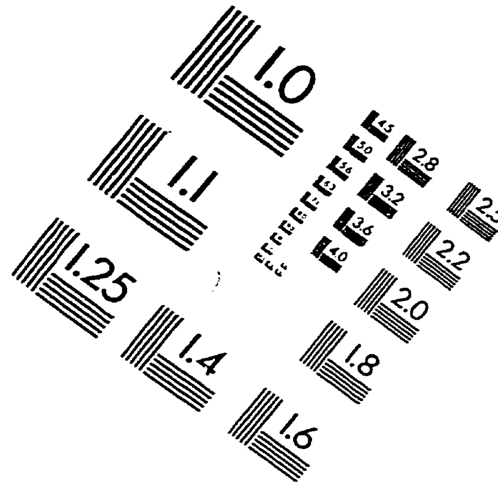

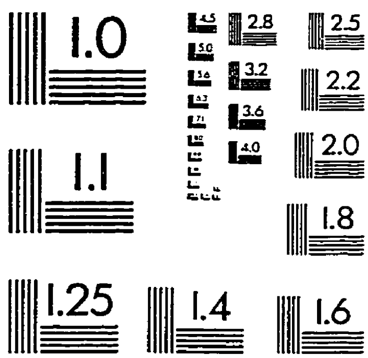

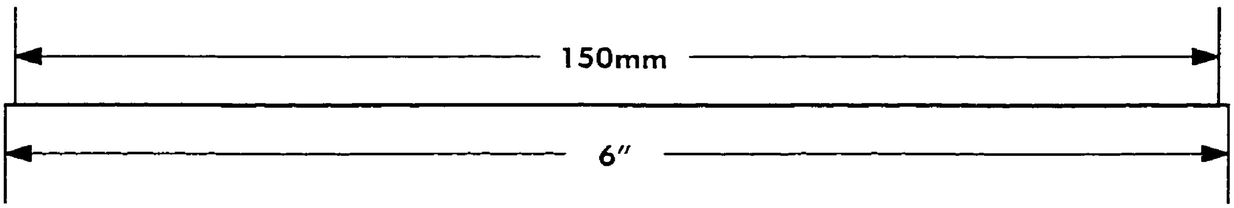

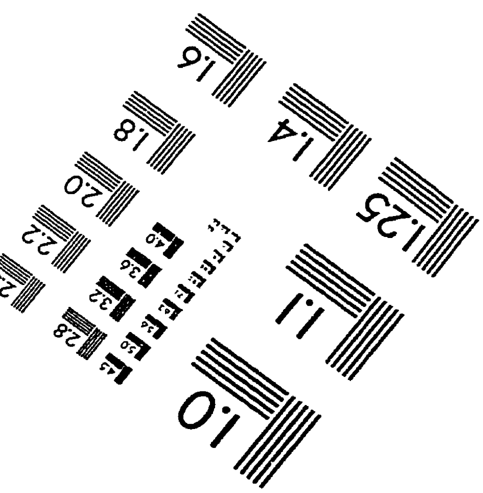

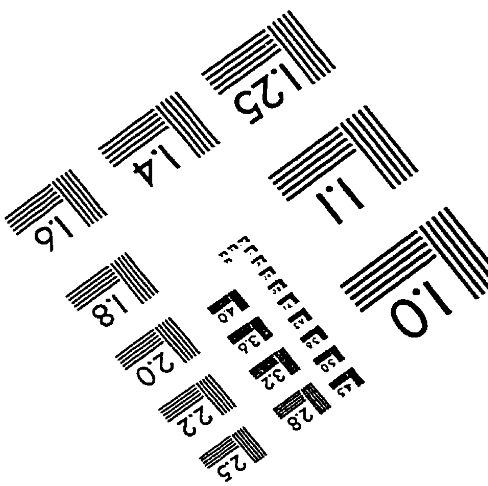

APPLIED IMAGE . Inc
1653 East Main Street
Rochester, NY 14609 USA
Phone: 716/482-0300
Fax: 716/288-5989